

NASA/TM-20230003630



H₂O Electrolysis With Impure Water Source—Final Report

Kenneth A. Burke
Glenn Research Center, Cleveland, Ohio

March 2023

NASA STI Program . . . in Profile

Since its founding, NASA has been dedicated to the advancement of aeronautics and space science. The NASA Scientific and Technical Information (STI) Program plays a key part in helping NASA maintain this important role.

The NASA STI Program operates under the auspices of the Agency Chief Information Officer. It collects, organizes, provides for archiving, and disseminates NASA's STI. The NASA STI Program provides access to the NASA Technical Report Server—Registered (NTRS Reg) and NASA Technical Report Server—Public (NTRS) thus providing one of the largest collections of aeronautical and space science STI in the world. Results are published in both non-NASA channels and by NASA in the NASA STI Report Series, which includes the following report types:

- TECHNICAL PUBLICATION. Reports of completed research or a major significant phase of research that present the results of NASA programs and include extensive data or theoretical analysis. Includes compilations of significant scientific and technical data and information deemed to be of continuing reference value. NASA counter-part of peer-reviewed formal professional papers, but has less stringent limitations on manuscript length and extent of graphic presentations.
- TECHNICAL MEMORANDUM. Scientific and technical findings that are preliminary or of specialized interest, e.g., “quick-release” reports, working papers, and bibliographies that contain minimal annotation. Does not contain extensive analysis.
- CONTRACTOR REPORT. Scientific and technical findings by NASA-sponsored contractors and grantees.
- CONFERENCE PUBLICATION. Collected papers from scientific and technical conferences, symposia, seminars, or other meetings sponsored or co-sponsored by NASA.
- SPECIAL PUBLICATION. Scientific, technical, or historical information from NASA programs, projects, and missions, often concerned with subjects having substantial public interest.
- TECHNICAL TRANSLATION. English-language translations of foreign scientific and technical material pertinent to NASA's mission.

For more information about the NASA STI program, see the following:

- Access the NASA STI program home page at <http://www.sti.nasa.gov>
- E-mail your question to help@sti.nasa.gov
- Fax your question to the NASA STI Information Desk at 757-864-6500
- Telephone the NASA STI Information Desk at 757-864-9658
- Write to:
NASA STI Program
Mail Stop 148
NASA Langley Research Center
Hampton, VA 23681-2199

NASA/TM-20230003630



H₂O Electrolysis With Impure Water Source—Final Report

Kenneth A. Burke
Glenn Research Center, Cleveland, Ohio

National Aeronautics and
Space Administration

Glenn Research Center
Cleveland, Ohio 44135

March 2023

Trade names and trademarks are used in this report for identification only. Their usage does not constitute an official endorsement, either expressed or implied, by the National Aeronautics and Space Administration.

Level of Review: This material has been technically reviewed by technical management.

H₂O Electrolysis With Impure Water Source—Final Report

Kenneth A. Burke
National Aeronautics and Space Administration
Glenn Research Center
Cleveland, Ohio 44135

1.0 Executive Summary

This Phase III final report summarizes the Phase I research and development work performed during the IRAD FY 2018-Cycle 1, Stage C-Phase I project March 15, 2018 through August 17, 2018 and during the Phase II continuation request which funded the research and development November 26, 2018 through September 30, 2019. A Phase III proposal was accepted to continue the technology development, but due to the unavailability of the Principal Investigators to complete the proposed Phase III work, the Phase III project was re-scoped to complete a final report on the research and development work that was previously completed as a wrap-up of this IRAD project.

The original objective of this research and development effort was to design, build and test a water electrolyzer that can directly use contaminated water. The contaminated water would contain minerals/salts expected from Lunar/Martian regolith or terrestrial lake/ocean water. The effort was to establish the feasibility of developing an alkaline water electrolysis cell based on the unique configuration tested by this investigator 38 years ago. The cell tested in 1984 used a potassium hydroxide electrolyte that was restrained within an asbestos separator. The configuration to be developed will be based on alkaline ion exchange membrane technology. A single cell was built and tested to establish the feasibility of this approach with a goal of >100 hr of operation.

A single cell was built and tested using both deionized water and a contaminated water mixture that simulated a Mars water mixture. The cell configuration was shown to be tolerant of water mixtures contaminated with non-volatile contaminants. The water did contain dissolved gases from the laboratory air, and these did not affect performance. The cell performance was satisfactory, operating at greater than 150 mA/cm² and under 1.9 VDC at 50 °C.

2.0 Goal/Gap

State of the Art H₂O electrolyzers require ultra-pure water be used to prevent contamination and degradation of the electrolysis electrodes. None of the water sources NASA is expecting to harvest or recover as part of its exploration efforts, meet this high purity, and therefore additional water purification is required. An electrolysis approach that can accept impure water can mitigate or eliminate this requirement improves the robustness of life support or ISRU equipment. An innovative cell design proposed by the Principal Investigator was designed and built along with the test rig to do the testing of this type of cell.

The Phase II goal was to complete the testing originally planned for Phase I and augment this with testing of a multicell electrolysis cell stack. The testing would also generate the parametric data needed for scale up, and determine where improvements in the design can be achieved. To accomplish this, a safety permit process and the original Phase I >100 hr of single cell operation must be completed. A multicell stack must be fabricated and tested at conditions envisioned for NASA missions. Engagement of the NASA life support, ISRU and energy storage groups will be needed to assist in identifying these conditions.

3.0 Approach/Innovation

The approach was to build and test innovative water electrolysis technology that could directly use the impure water expected from NASA's water mining/recovery during planetary exploration and settlement. The innovative single cell is conceptually shown in Figure 1. The cell has three separated compartments, one compartment for the evolved oxygen (and water vapor in the oxygen), one compartment for the evolved hydrogen (and water vapor in the hydrogen), and one compartment for water (with contaminants). The water compartment is separated from the hydrogen compartment by a porous hydrophobic membrane that permits water vapor to permeate the membrane, but which prevents the transport of bulk liquid water (and contaminants) from the water compartment to the hydrogen compartment. The permeation of water vapor is equivalent to the distillation of water from a contaminated bulk liquid water stream. The liquid water stream also acts as the cooling stream preventing the cell from over-heating.

The results of the Phase II testing of this cell configuration demonstrated the feasibility of operating with contaminated water. This represents new patentable technology. Future work to further develop this technology will consist of cell improvements to improve performance, improving the test rig to allow unattended longer operation, testing with other relevant contaminated water mixtures, analyzing the data, and communicating the results to NASA customers.

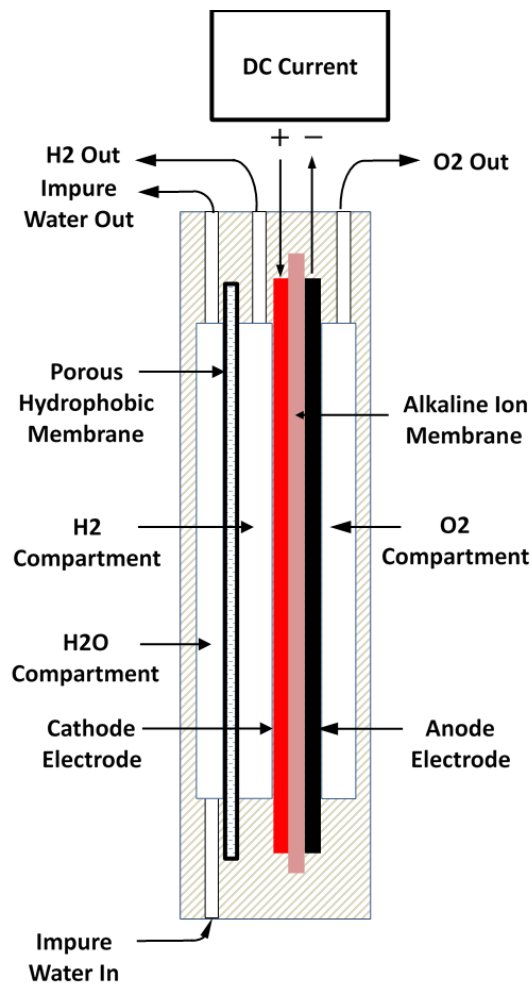


Figure 1.—Conceptual Cell Diagram.

4.0 Results/Knowledge Gained/Technology Transfer

4.1 Testing Summary

Table I summarizes the single cell testing that was done. Table I lists the date of each test, the operating time, maximum cell temperature, maximum current during the test, the quality of the water used by the cell and the alkaline membrane used. A total of 30.15 hr of operation was completed. A more detailed description of each test is contained in Appendix C—Test Results.

4.2 Hydrogen and Oxygen Gas Flow Results

During the tests that were run on 03/27/19 the gases exiting the cell were measured with a 25 cc soap bubble flow meter which provides highly accurate measurement of the small gas flows. The oxygen and hydrogen gas flows were measured and compared to the theoretical gas flows that were expected based upon complete utilization of the electrical current. The comparison of the measured flow to the theoretical flow listed as a percentage of the theoretical is referred to as “current efficiency”. A 100% current efficiency means that every electron passed through the cell goes to producing. Table II and Table III show the measured flows, the theoretical flows, and the calculated current efficiencies. The oxygen flow showed essentially 100% current efficiency while the hydrogen flow showed slightly less (96.2 to 97.6%). Gas flow measurements were also taken during the tests run on 07/19/19, 07/23/19, and 08/01/19 with similar results. More detailed information about the flow measurement results is available in Appendix C—Test Results.

TABLE I.—TEST SUMMARY

Date	Operating time, hh:mm:ss	Max current, A	Max temperature, °C	Water quality	Membrane
3/27/2019	3:49:00	6.3	40	Deionized	Sustainion
3/28/2019	0:02:00	0.2	21	Deionized	Sustainion
3/28/2019	2:23:00	1.8	41	Deionized	Sustainion
7/17/2019	0:50:00	1.247	36.63	Deionized	Sustainion
7/18/2019	3:01:00	6.676	47.795	Deionized	Sustainion
7/23/2019	3:32:20	10.175	51.715	Deionized	Sustainion
7/26/2019	2:27:00	7.165	51.63	Deionized	Sustainion
7/30/2019	2:14:00	13.5	50.57	Contaminated	Sustainion
8/1/2019	4:57:00	16.5	52.83	Contaminated	Sustainion
8/6/2019	2:43:00	15.657	50.85	Contaminated	Sustainion
10/2/2019	1:07:40	0.311	45.515	Contaminated	W7energy
10/3/2019	1:30:10	1.236	47.125	Contaminated	W7energy
10/23/2019	1:34:05	1.26	46.155	Contaminated	W7energy

TABLE II.—ANODE (OXYGEN) SIDE

Cell Current Amperes	Cell Current Density mA/cm ²	Calculated Water Use ml/min	Calculated Oxygen Flow gms/min	Calculated Oxygen Flow cm ³ /min	Calculated Anode Total Flow cm ³ /min	Calculated Time to flow 25cc seconds	Measured Time to flow 25cc seconds	Estimated Current Efficiency %
5.2	52	0.029	0.03	20.42	21.08	71.17	70.55	100.88
5.6	56	0.031	0.03	22.28	23.00	65.21	66.22	98.48
5.7	57	0.032	0.03	22.68	23.41	64.07	64.52	99.30

TABLE III.—CATHODE (HYDROGEN) SIDE

Cell Current Amperes	Cell Current Density mA/cm ²	Calculated Water Use ml/min	Calculated Hydrogen Flow gms/min	Calculated Hydrogen Flow cm ³ /min	Calculated Cathode Total Flow cm ³ /min	Calculated Time to flow 25cc seconds	Measured Time to flow 25cc seconds	Estimated Current Efficiency %
5.2	52	0.029	0.003	41.38	42.72	35.11	36.00	97.54
5.3	53	0.030	0.003	42.18	43.54	34.45	35.81	96.21
5.4	54	0.030	0.003	42.97	44.36	33.81	35.07	96.42
5.5	55	0.031	0.003	43.77	45.18	33.20	34.36	96.62

4.3 Rubber Gasket Extrusion Into Gas Exits

The rubber gaskets that provided the gas sealing were extruding into the thin O₂ and H₂ exit grooves blocking the gas from exiting. This was observed during the first single cell build. The design was modified by cutting the grooves into the underlying cell frame material and provide a “cover” over these grooves to prevent the extrusion. This solved the issue.

4.4 Endplate Stresses

After the test run 03/28/19 it was noticed that the endplate on the cathode side of the cell had developed a crack. This endplate was replaced, and the cell reassembled, but before testing resumed the endplate on the anode side of the cell severely cracked (Figure 2). Table IV shows the polyester material used for the endplates had a low impact strength rating. New endplates were fabricated using polycarbonate and 20% glass filled polycarbonate both of which had a better impact strength rating which reduces the likelihood of cracking. Although some endplate cracking was still observed on one cell build, it was very minor.

4.5 Deionized Water vs. Contaminated Water

Tests were done 7/30/19, 8/1/19, 8/6/19, 10/2/19, 10/3/19, and 10/23/19 with a contaminated water mixture that was provided by the group at NASA working Mars In-Situ-Resource- Utilization (ISRU) technology. The composition of the water mixture is shown in Table V.

The tests done on 7/30/19, 8/1/19, and 8/6/19 used the same alkaline membrane as tests don earlier, so these test offer the best comparison with earlier tests that used deionized water. The results from 7/23/19 are shown in Figure 3. During this test as the cell temperature was increased and the water diffuses more rapidly to the cathode, allowing the current to be increase without drying out the cell. During this test the current reached a maximum of 10.15 A (101 mA/cm²) at a voltage of 2.1 VDC. The deionized water tests were done first to establish performance with purified water.

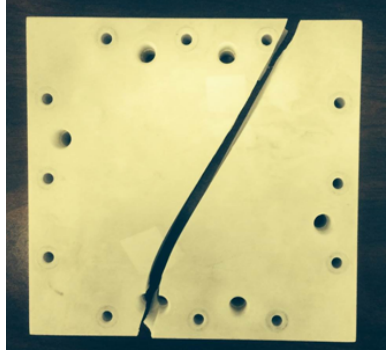


Figure 2.—Cracked Anode Endplate.

TABLE IV.—MATERIAL PROPERTIES OF ELECTROLYZER ENDPLATE MATERIALS

Material	Polyester Plastic	Polycarbonate Plastic	Polycarbonate Plastic 20% Glass Filled
Impact Strength	0.65 ft.-lbs./in.	2 ft.-lbs./in.	2.06 ft.-lbs./in.
Impact Strength Rating	Poor	Good	Good
Tensile Strength	11,600 psi	9,100-9,500 psi	12,000 psi
Tensile Strength Rating	Good	Good	Excellent

TABLE V.—MARS ISRU WATER MIXTURE

Reagent Name	Formula	Conc. g/L
Water	H ₂ O	
Calcium Carbonate	CaCO ₃	1.6
Magnesium Carbonate	MgCO ₃	0.8
Magnesium Sulfate Heptahydrate	MgSO ₄ * 7H ₂ O	1.2
Potassium Chloride	KCl	0.032
Sodium Bicarbonate	NaHCO ₃	0.12
Calcium Chlorate Tetrahydrate	Ca(ClO ₄) ₂ *4H ₂ O	0.46
Magnesium Chlorate Hexahydrate	Mg(ClO ₄) ₂ *6H ₂ O	0.332

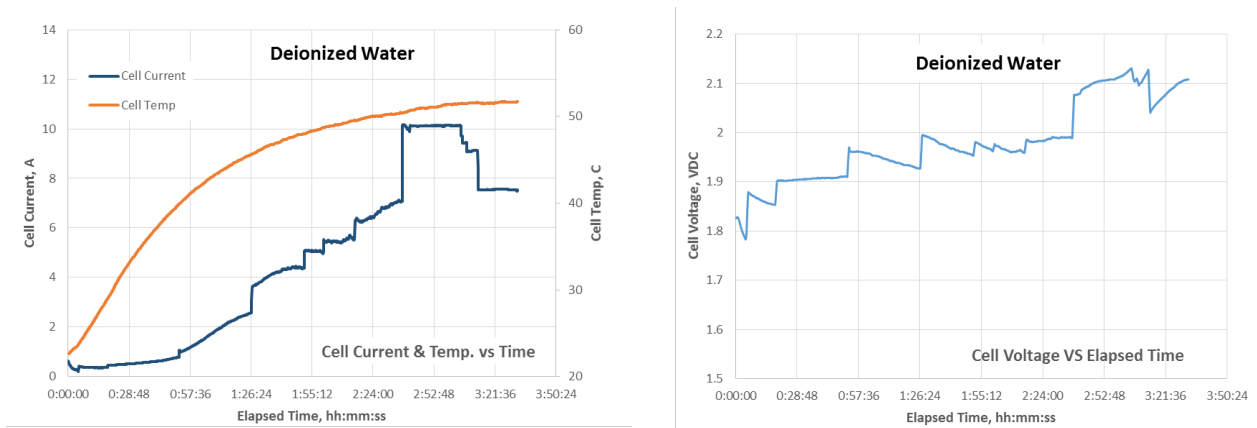


Figure 3.—Deionized Water Test 7/23/19.

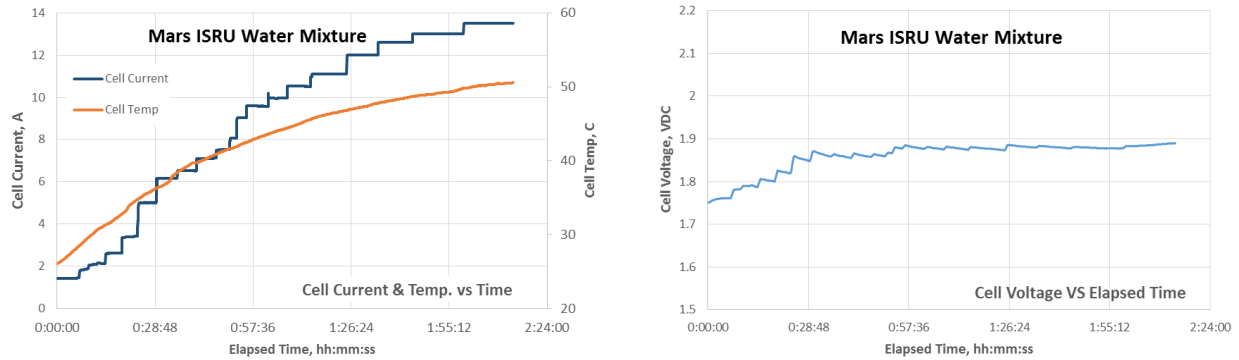


Figure 4.—Contaminated Water Test 7/30/19.

A similar test was done 7/30/19 with the simulated Mars ISRU water mixture. The results from this test are shown in Figure 4. Like the deionized water test as the cell temperature increases the water diffuses more rapidly to the cathode, allowing the current to be increase without drying out the cell. The maximum current reached was about 13.5 A (135 mA/cm²) at a voltage of 1.9 VDC. At 10 A the cell voltage was 1.88 V which is lower (better) than in the deionized water test where at 10 A the voltage was 2.1 V. The contaminated water performance was better than that achieved with deionized water. This was the case for other tests done with contaminated water. Details of the tests are found in Appendix C—Test Results.

4.6 Technology Transfer

A NASA “Disclosure of Invention and New Technology Report”, nf 1679 was completed and given to the GRC legal office. No publications have been produced for this work to date.

5.0 Technology Maturation and Infusion Opportunities

5.1 Technology Maturation

The technology maturation and transition of this technology could be supported by these additional steps:

1. Address the unresolved technology issues discovered by the development work of this technology done to date. This is discussed in more detail in Sections 4.0 and 7.0 of this final report.
2. Suggest/promote the incorporation and integration of this technology with other life support and ISRU technologies currently being investigated and developed by NASA and commercial space contractors.
3. Suggest/promote this technology to commercial hydrogen development parties as a means to produce low cost hydrogen from impure water sources such as seawater and other surface water sources.

5.2 Technology Infusion

A portion of the work completed was testing this technology with a simulated Mars water composition suggested by the NASA ISRU working group. This described further in Sections 4.0 and 7.0 of this final report.

The principal people engaged by the Principal Investigator were:

1. Diane Linne, NASA GRC—In-Situ-Resource-Utilization projects
2. Gerald Sanders, NASA JSC—In-Situ-Resource-Utilization projects
3. Danial Barta, NASA JSC—NASA Life Support projects

6.0 Potential Impact

Water is a critical resource needed for manned exploration and long term settlement of planetary bodies such as the Moon and Mars. Water is available as a recovery product from life support recycling. Water is also available from water mining/recovery from planetary subsurface ice on the Moon or Mars. The quality of the water is not suitable for use in state-of-the-art water electrolyzers that could convert the water to needed oxygen and hydrogen. The recovered water is expected to contain significant amounts of contaminants that would poison state-of-the-art electrolyzers.

Water electrolyzers that could directly use impure water without the use of purification equipment could enable, enhance or otherwise influence the trade space for future NASA missions.

7.0 Outcome

The conclusions and state of knowledge from this project are:

1. The cell that was designed, built and tested established the feasibility and practicality of operating an alkaline membrane electrolyzer based on providing water to the cell in the form of water vapor rather than direct contact with liquid water. Moreover, operating the cell with water vapor provides substantial protection of the cell from water contaminants expected in the water NASA produces from planetary surface water mining/recovery.
2. Liquid water flowing through the cell not only provides the source of water vapor, but also provides the means to heat or cool the cell.
3. The gas flows measured demonstrate a very high current efficiency (100% for oxygen and 95+% for hydrogen. The lower hydrogen value may be due to hydrogen leaving the cell in the form of hydrogen dissolved in the liquid water leaving the cell.
4. Gasket seal in the current design result in higher compression loads needed for sealing. The higher compression loads have the undesirable consequences of rubber extrusion into the gas exits and over-stressed endplates that are susceptible to cracking. A cell redesign that used o-ring seals would prevent both of these undesired effects.
5. More experience with alkaline membrane technology is needed to optimize this critical part of the electrolyzer. Handling, cutting, assembly, and pre-conditioning are areas of additional investigation. Since 2019 additional membrane suppliers that produce membranes with of different chemical composition are available.
6. A cell redesign that would reduce the diffusion distance required of the water vapor would increase the electrical current capability of the cell. Also, increasing the cell temperature above 50 °C would also increase the electrical current capability of the cell.
7. Improving the test rig to allow for unattended testing would allow more operating hours to be achieved faster. This would facilitate the investigation of long term performance stability.

8.0 External Partnerships

There were no external partnerships that were part of this IRAD project.

9.0 GRC Team Members

Kenneth A. Burke was the principal investigator for this IRAD project. He was the original innovator of this technology. He designed, built and tested the electrolysis cells. He also was the liaison between this project and NASA's ISRU customers. Charles Castle, GESS III Vantage Partners, was the Mechanical Designer.

10.0 Impact Assessment

This IRAD project completed the Phase II work in late 2019, and was accepted for continuation in January 2020. Work had just begun when the COVID-19 pandemic caused the shutdown of nearly all NASA GRC work (including this project). Over two years later in spring of 2022 this project was selected for a re-start. At that time the project was proposed to be done by the original Principal Investigator and another Co-Principal Investigator that was interested in the technology. Unfortunately, both investigators had become involved other NASA projects that severely restricted their availability to perform the work for the proposed Phase III effort, and because little progress had been made, in October 2022 the Phase III project was rescoped and the Principal Investigator was asked to complete a final report documenting the work done to date for this IRAD project.

Appendix A.—Electrolysis Cell/Stack Design

A.1 Cell/Stack Design

[Figure A1](#) shows the electrolysis cell diagram. Impure water enters the water compartment, flows through the water compartment and exits the electrolysis cell. Some of the water diffuses through the porous hydrophobic membrane. Liquid water does not penetrate through the porous hydrophobic membrane due to the membrane's average pore size and the membrane's hydrophobicity. The diffusion of water vapor through the membrane is essentially a distillation of water. Low vapor pressure water contaminants such as dissolved salts in the water are retained in the liquid water exiting the cell.

The water vapor that diffuses through the hydrophobic membrane diffuses to the electrolysis cell cathode of the Membrane Electrode Assembly where the water vapor molecules are split to form hydrogen and hydroxyl (OH⁻) ions (Equation 1). The hydroxyl ions are ionically conducted to the anode of the Membrane Electrode Assembly where oxygen, water, and electrons are generated (Equation 2). The electrons generated at the anode return to the DC Current power supply, completing the electrical circuit.

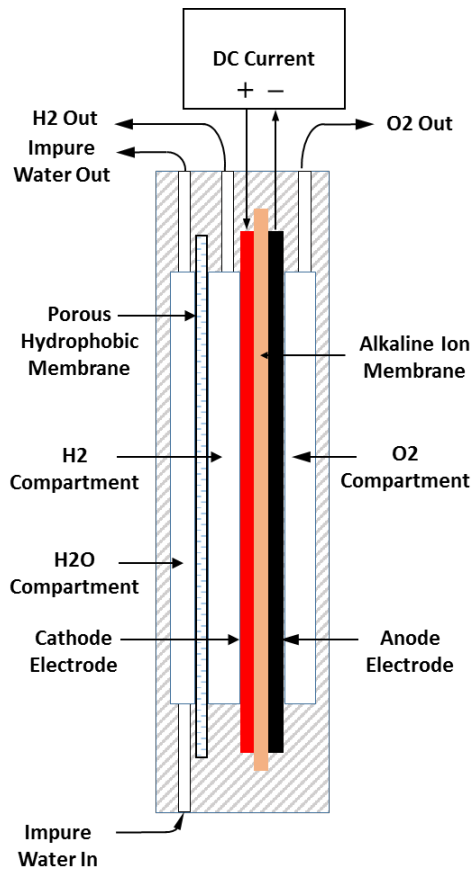
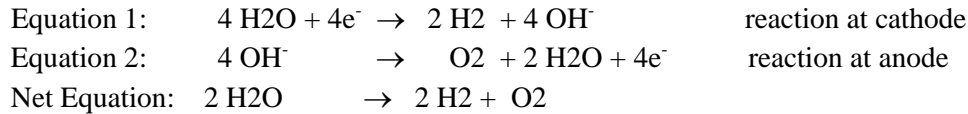


Figure A1.—Electrolysis Cell Diagram.

A.2 Membrane Electrode Assembly

The Membrane Electrode Assembly shown in Figure A2 consists of an anode electrode with its attached EPDM Gasket, a cathode electrode with its attached EPDM Gasket, and an anion exchange membrane sandwiched in between the two electrodes.

Each electrode is glued to its mating EPDM gasket using a hot melt polyester glue. Attaching the gaskets to the electrodes prevents misalignment of these critical components during assembly. The anion exchange membrane is larger than the electrodes and is centered in such a way as to have some overlap with each electrode. The anion exchange membrane is required to be wet so that it lays flat against the electrodes and is pliable enough that the assembly process does not damage the membrane. The manifold holes in the EPDM gaskets provides the alignment with the other components of the electrolysis cell.

Figures A3, 4, 5, and 7 are dimensioned drawings of the EPDM Gasket, anion membrane, cathode and anode respectively. Figure A6 shows the cathode electrode with its EPDM gasket frame. CEC-120 is titled “PVDF Gasket” but the gasket was actually made of EPDM rather than PVDF. This is also the case for Figure A8 which shows the anode electrode with its EPDM gasket frame.

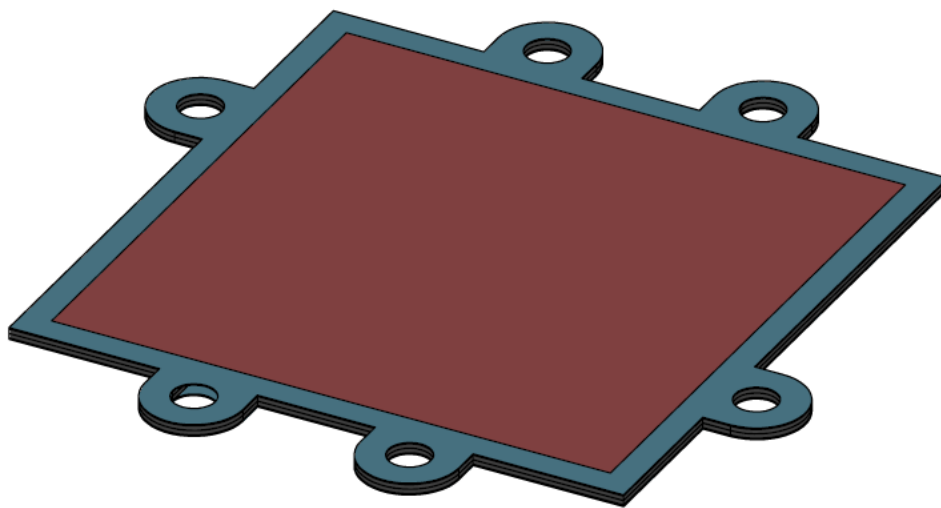


Figure A2.—Membrane Electrode Assembly.

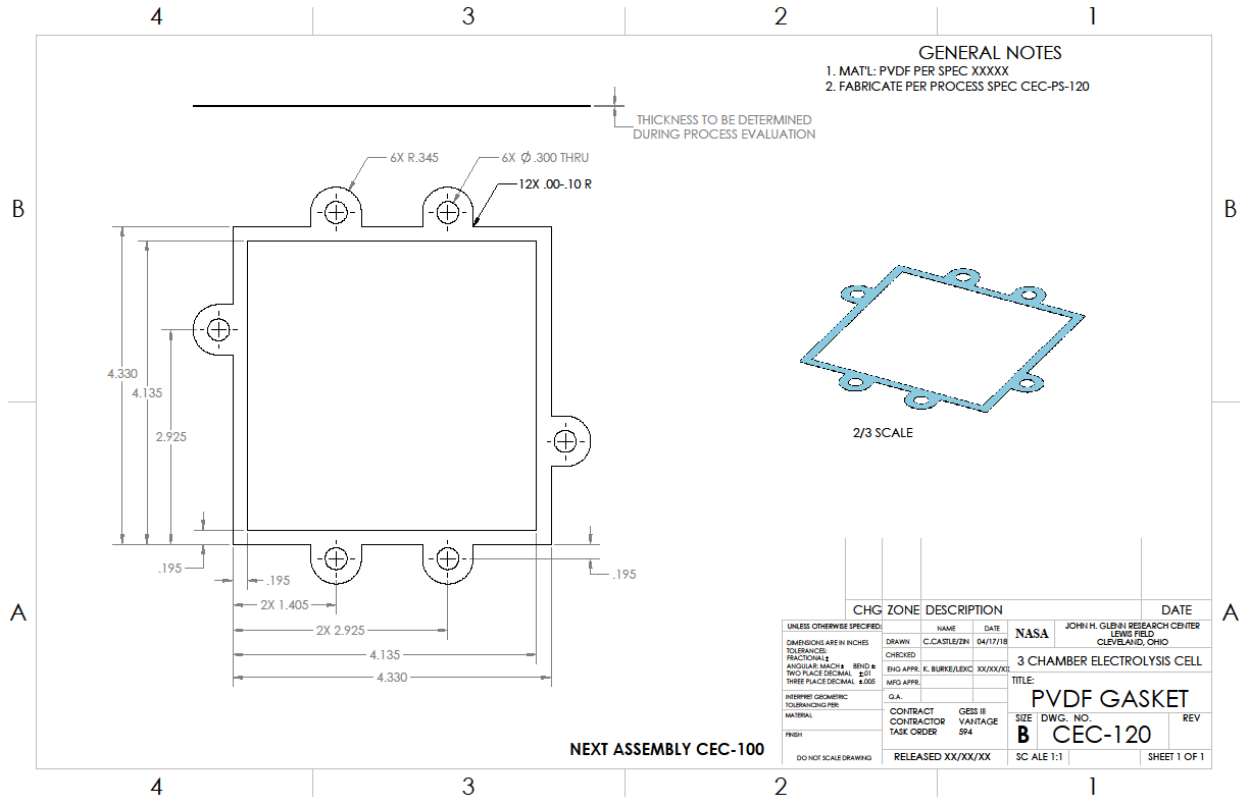


Figure A3.—PVDF Gasket CEC-120 Dimensioned Drawing.

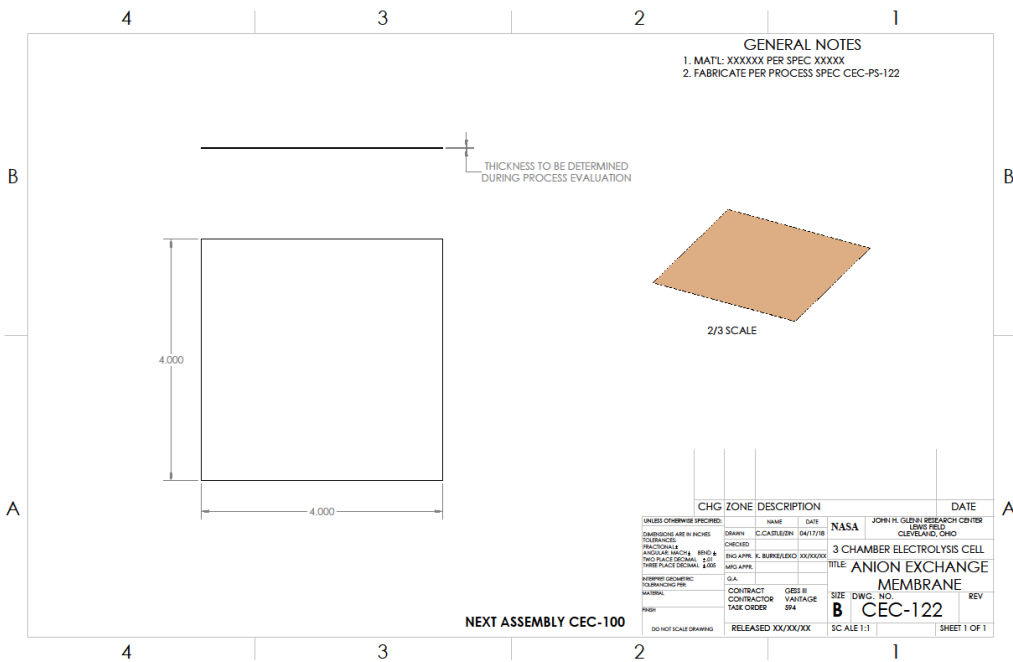


Figure A4.—Anion Exchange Membrane CEC-122 Dimensioned Drawing.

A.3 Flow Field Assembly

Figure A9 shows the porous PTFE membrane plate assembly. This assembly consists of the Garolite Separator (CEC-102), Water Manifold (CEC-101), Membrane Frame (CEC-105), Flow Field Mesh (CEC-128), and Porous PTFE Membrane (CEC-127). The parts CEC-102, 101, and 105 are glued together using a hot melt polyester glue which keeps the parts together and forms a leak tight seal between these parts. The water Flow Field mesh (CEC-128) is inserted into the Membrane Frame (CEC-105) and the Porous PTFE Membrane (CEC-127) is placed over the water Flow Field Mesh (CEC-128) and glued to the Membrane Frame using the hot melt polyester glue. This glued assembly is the Porous PTFE Plate Assembly shown in Figure A9.

The nickel cathode current collector (Perforated Nickel Foil CEC-104) is glued to the Porous PTFE Membrane Plate Assembly and the Flow Field Gasket (CEC-118) is glued to the top of the nickel cathode current collector. The parts CEC-104, 118, and the Porous PTFE Membrane Plate Assembly are glued together using a hot melt polyester glue which keeps the parts together and forms a leak tight seal between these parts. This glued assembly is shown in Figure A10 which also shows the Flow Field Mesh (CEC-119). The Flow Field Mesh conducts electrons from the cathode (hydrogen) electrode (CEC-123) (not shown in Figure A10) to the nickel cathode current collector (Perforated Nickel Foil CEC-104). The assembly shown in Figure A10 is the Flow Field Assembly (H2 Side) that is on the hydrogen side of the electrolysis cell.

Since only a single cell configuration was tested, there were two separate flow field assemblies used, one on the hydrogen side (Figure A10) and one on the oxygen side (Figure A11). In a multicell configuration the flow field assembly used would be the combination of the flow field assemblies shown in Figures A10 and A11. Figure A12 shows an exploded view of the multicell configuration flow field assembly. Figure A12 shows the flows of water, hydrogen, and oxygen in their respective cavities and manifolds.

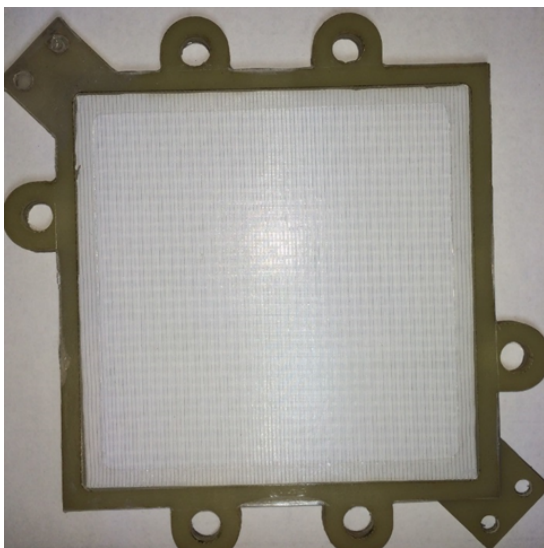


Figure A9.—PTFE Porous Membrane Plate Assy.

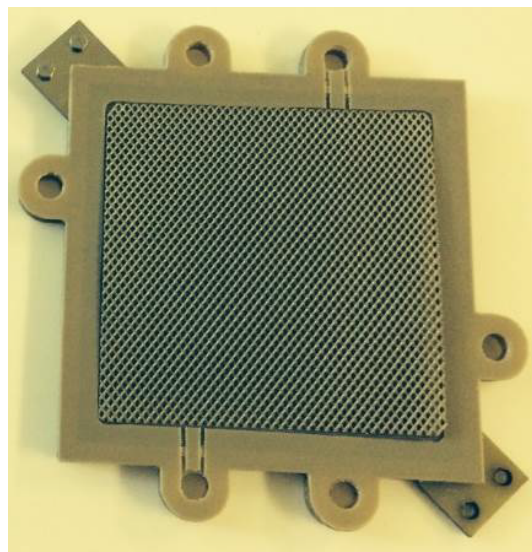


Figure A10.—Flow Field Assembly (H2 Side).

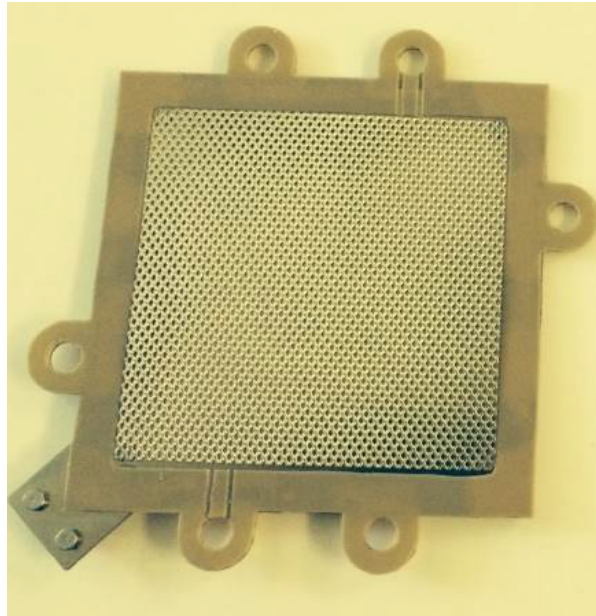


Figure A11.—Flow Field Assembly (O₂ Side).

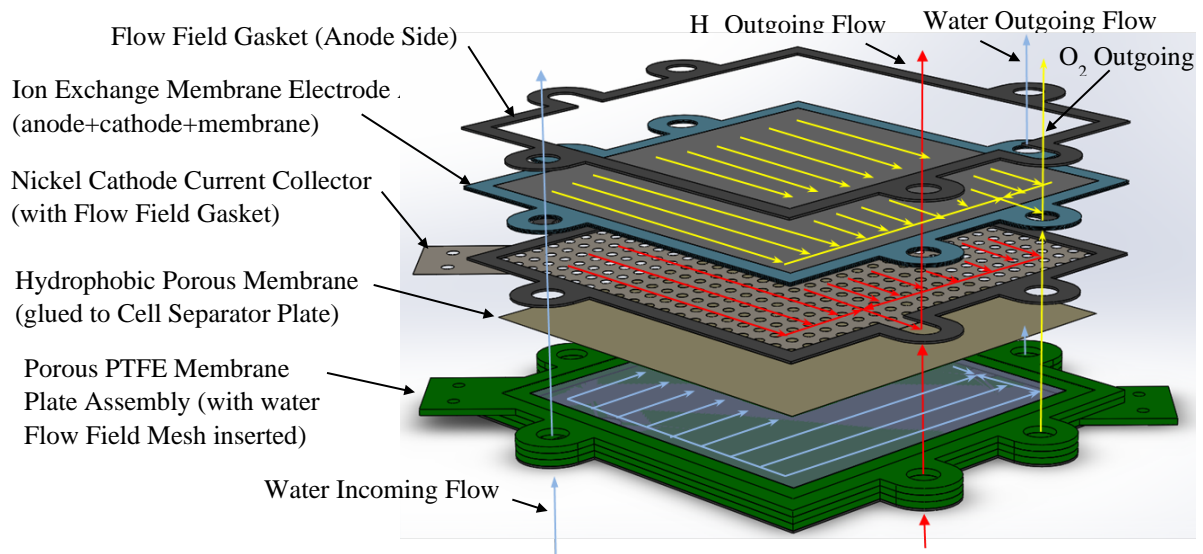


Figure A12.—Multicell Configuration of the Flow Field Assembly.

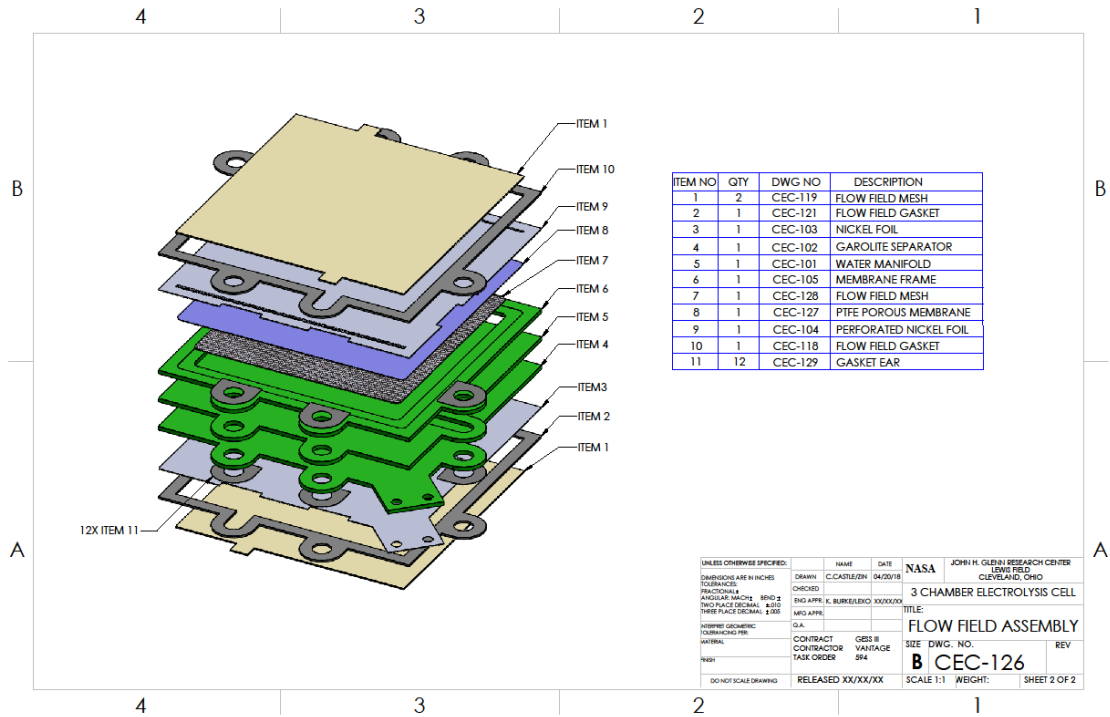


Figure A13.—Multicell Configuration Flow Field Assembly.

Figure A13 also shows an exploded view of the multicell configuration flow field assembly (CEC-126). Except for the Flow Meshes on the anode and cathode sides, the balance of the parts are glued together using a hot melt polyester glue. The polyester glue comes in a thin sheet form that is cut and placed between the various layers. The layers to be glued and the layer(s) of glue are placed into a press and heated to the softening/melting point of the glue (132 °C) with a compressive force of approximately 100 lb which bonds the layers together.

Figures A14 to A24 show the dimensioned drawings of the multicell flow field assembly components.

A.4 Cell Stack

Figure A25 shows the cell stack Electrolysis Assembly (CEC-100). The endplate at the anode side of the multicell cell stack is Endplate 1. Next to Endplate 1 is the O2 side Flow Field (shown in Figure A11). The anode (oxygen evolving) electrode (Figure A8) of a Membrane Electrode Assembly is next to Endplate 1. At the other end of the cell stack is the H2 side Flow Field (shown in Figure A10), and next to it the cathode side Endplate 2. The cell stack is squeezed together by threaded fasteners and spring washers. Figures A26 and A27 are dimensioned drawings of Endplate 1 and 2. Figure A28 shows a picture of an assembled single electrolysis cell.

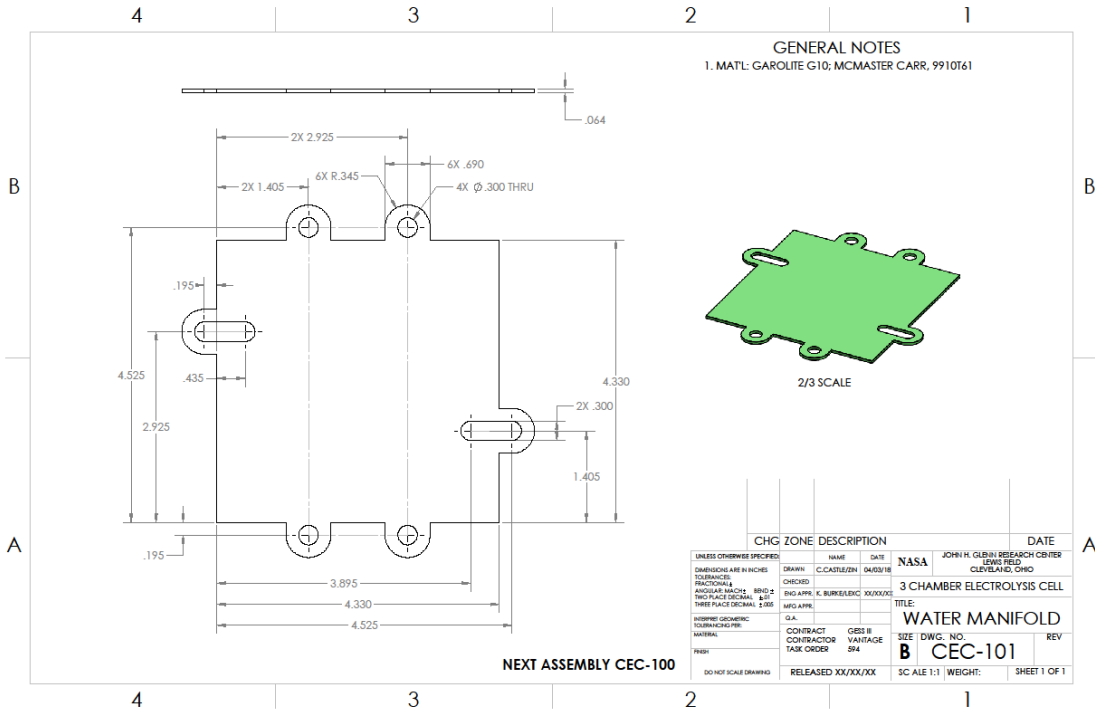


Figure A18.—Water Manifold (CEC-101) Dimensioned Drawing.

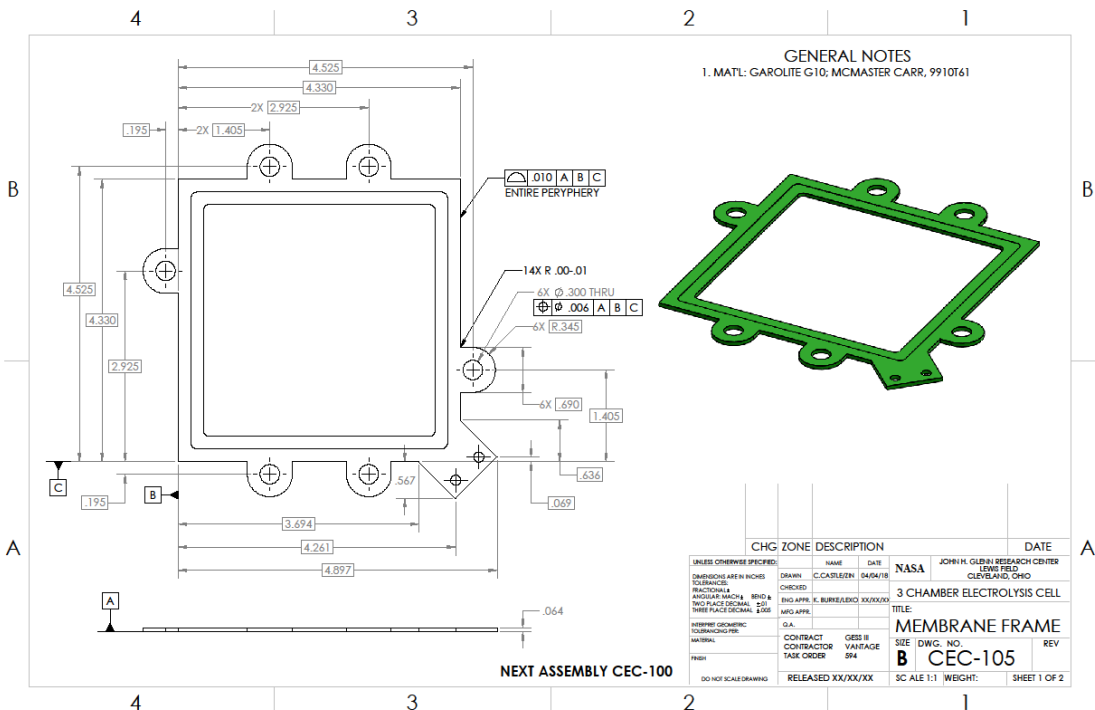


Figure A19.—Membrane Frame (CEC-105) Dimensioned Drawing.

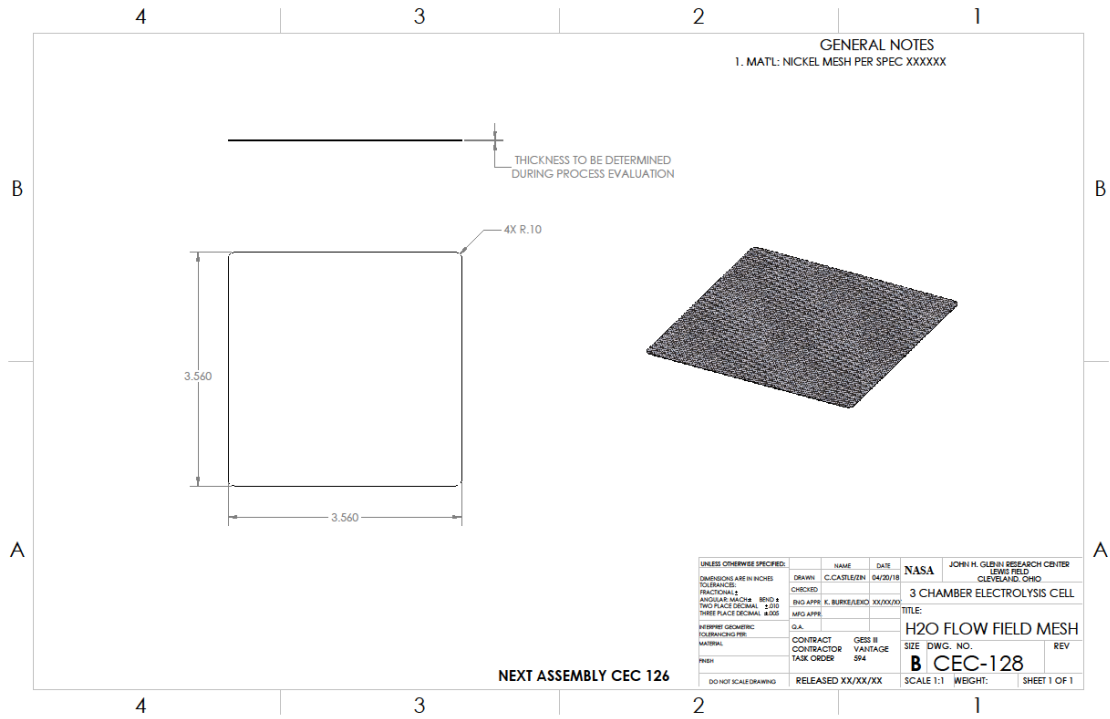


Figure A20.—H2O Flow Field Mesh (CEC-119) Dimensioned Drawing.

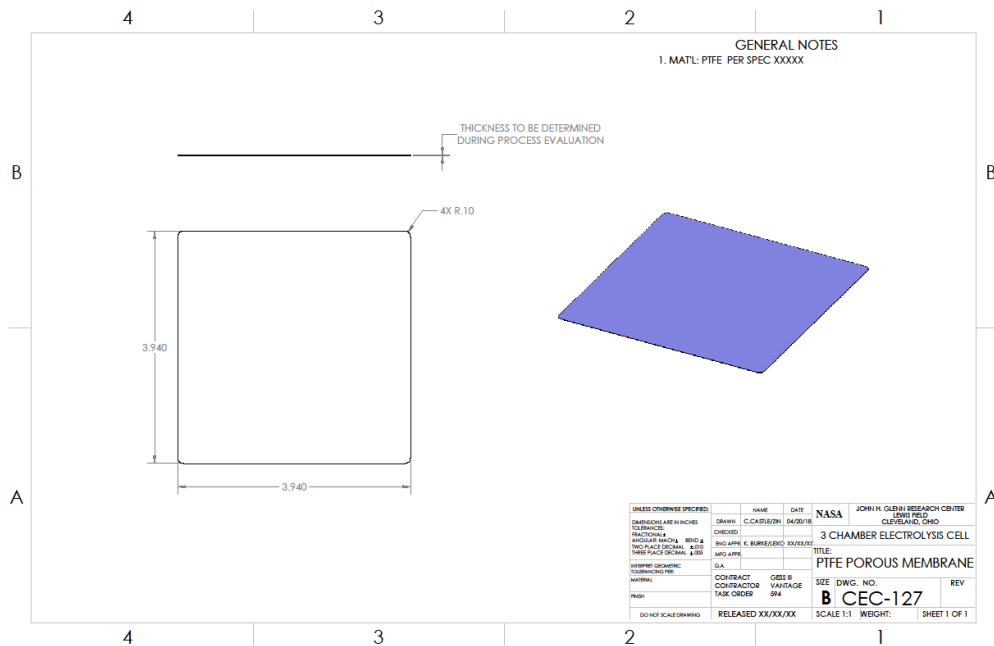


Figure A21.—PTFE Porous Membrane (CEC-127) Dimensioned Drawing.

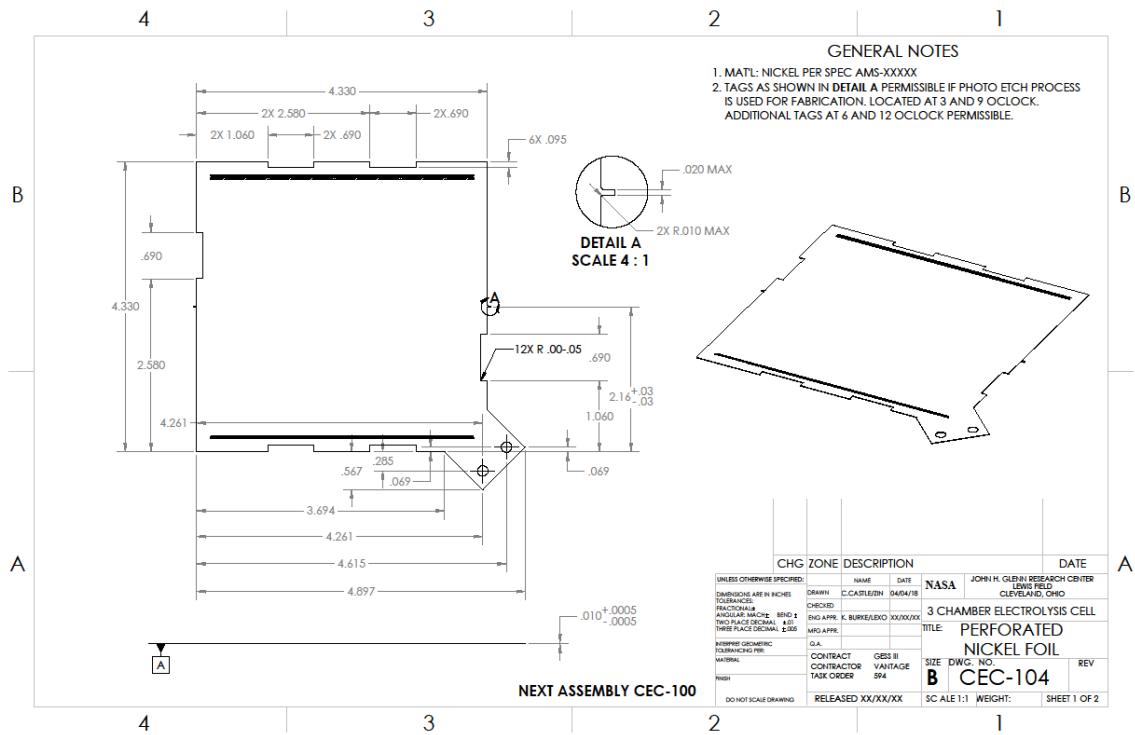


Figure A22.—Perforated Nickel Foil (CEC-104) Dimensioned Drawing.

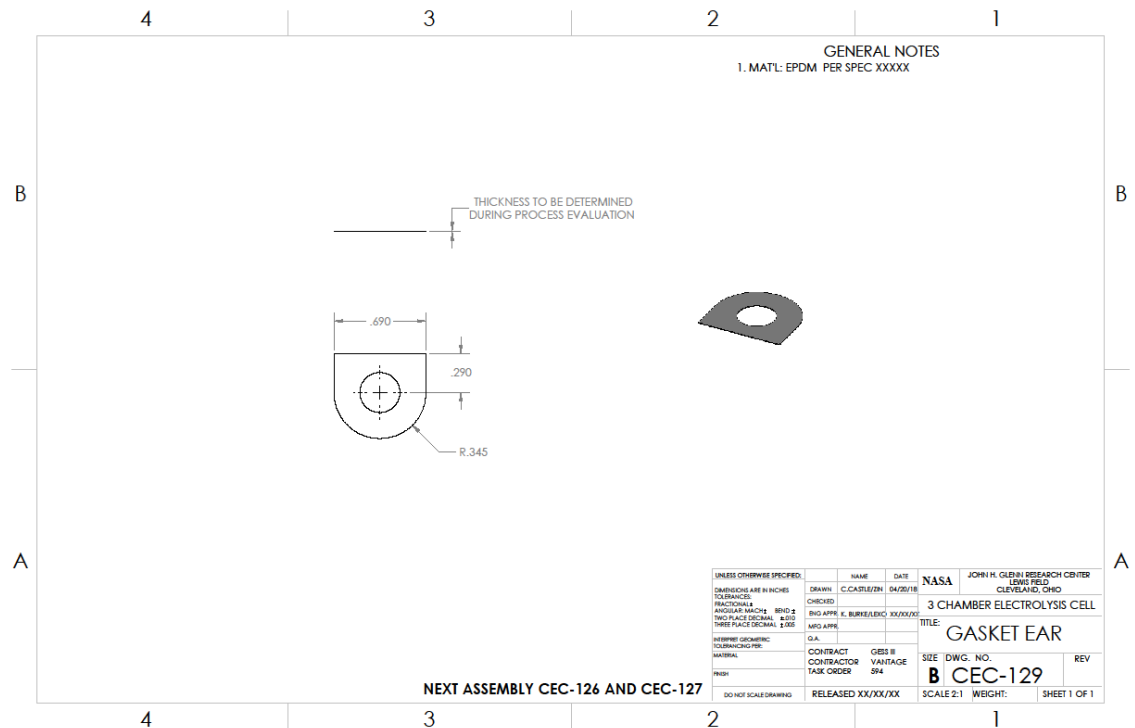


Figure A23.—Gasket Ear (CEC-129) Dimensioned Drawing.

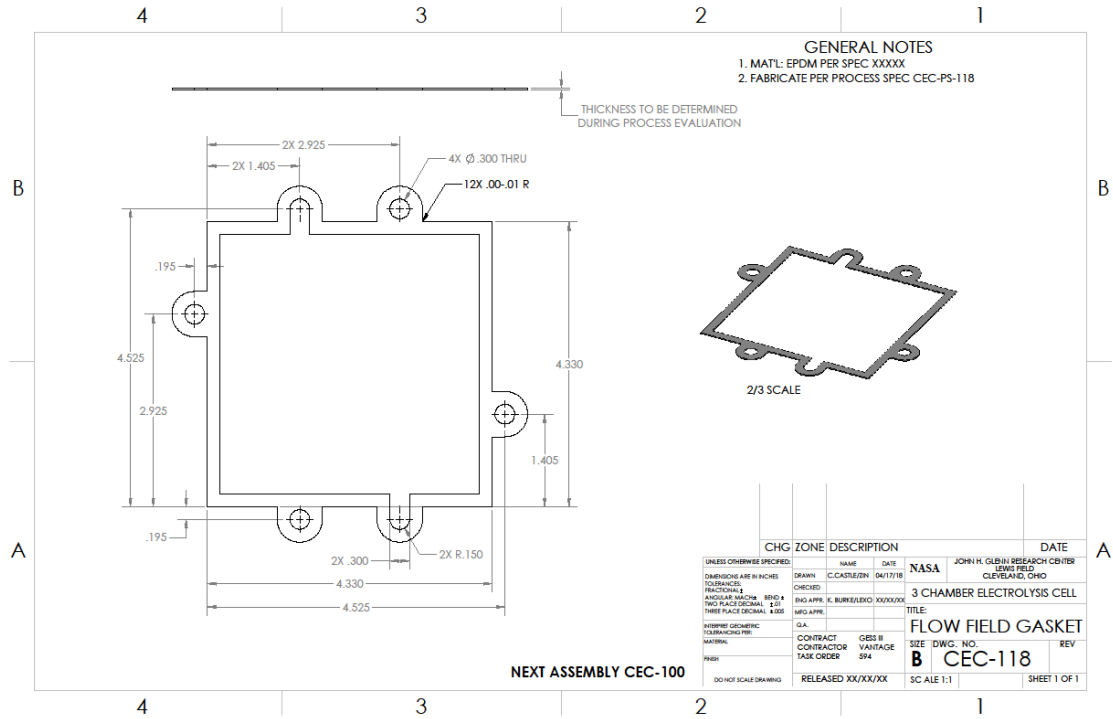


Figure A24.—Flow Field Gasket (CEC-118) Dimensioned Drawing.

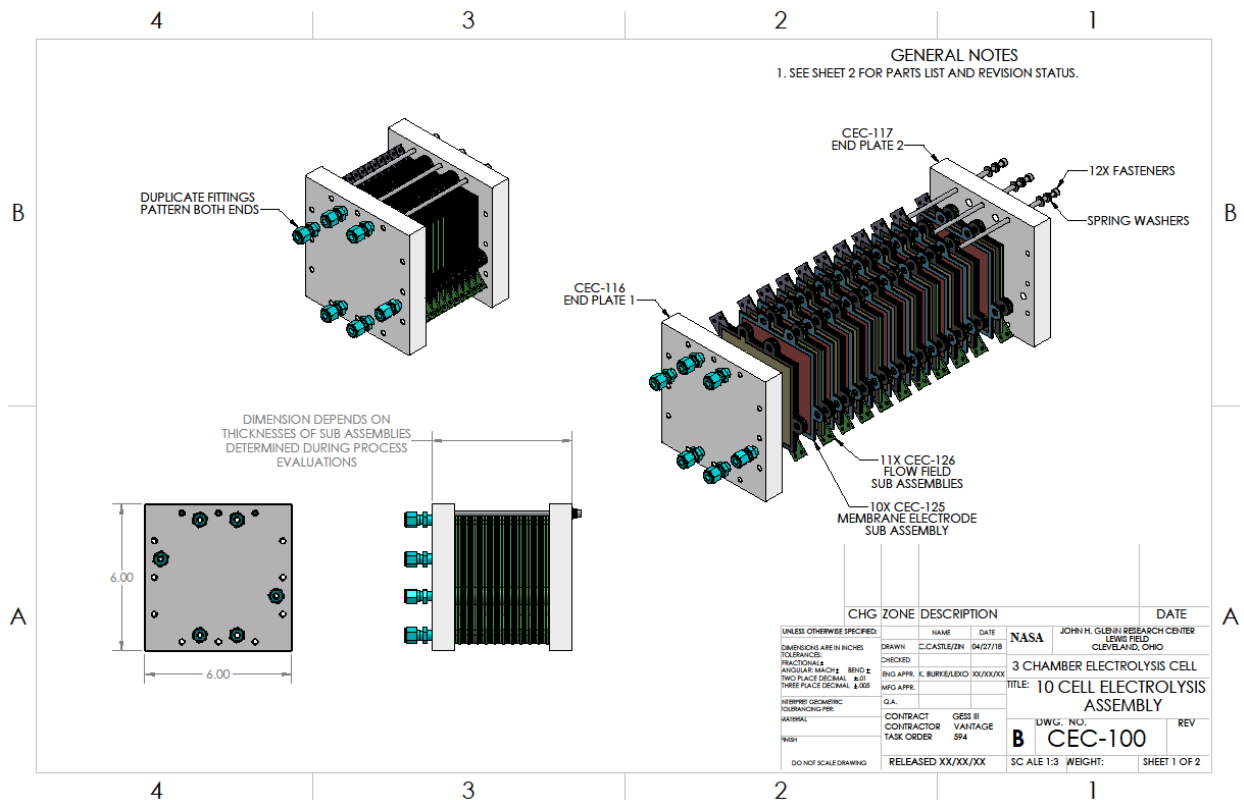


Figure A25.—Multicell Electrolysis Assembly (CEC-100) Dimensioned Drawing.

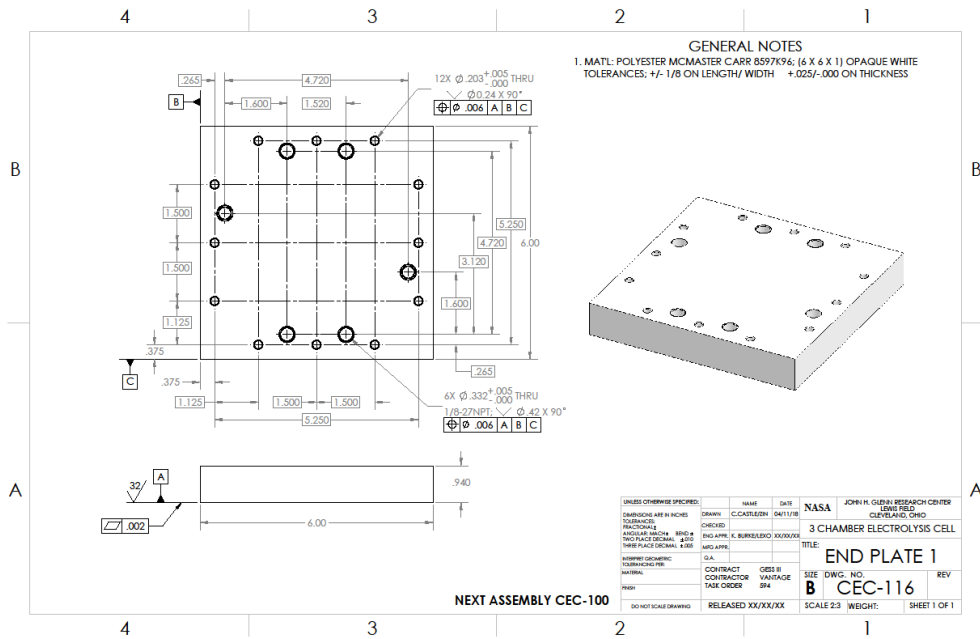


Figure A26.—Anode End Plate 1 (CEC-116) Dimensioned Drawing.

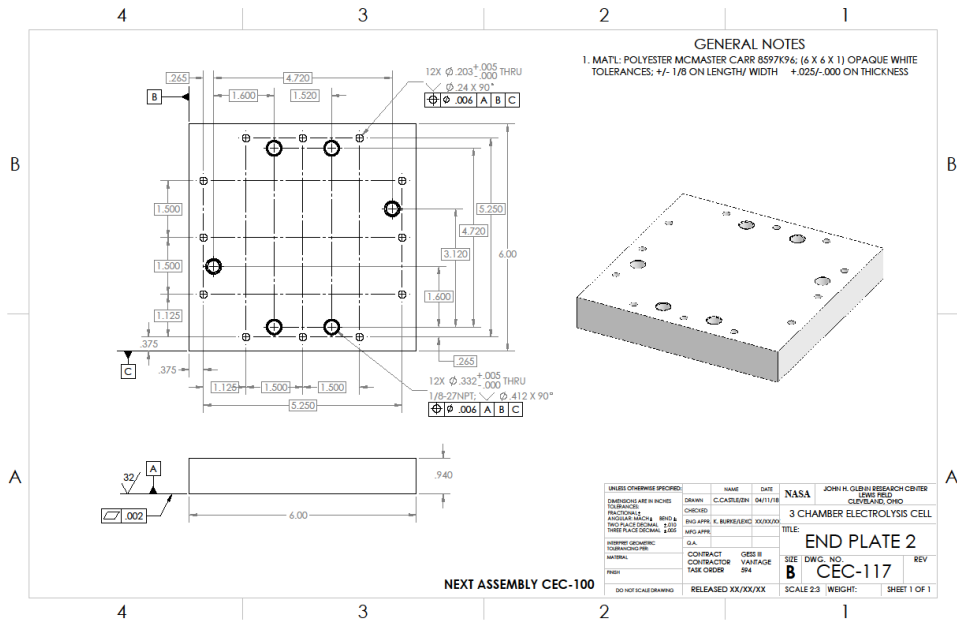


Figure A27.—Cathode End Plate 2 (CEC-118) Dimensioned Drawing.

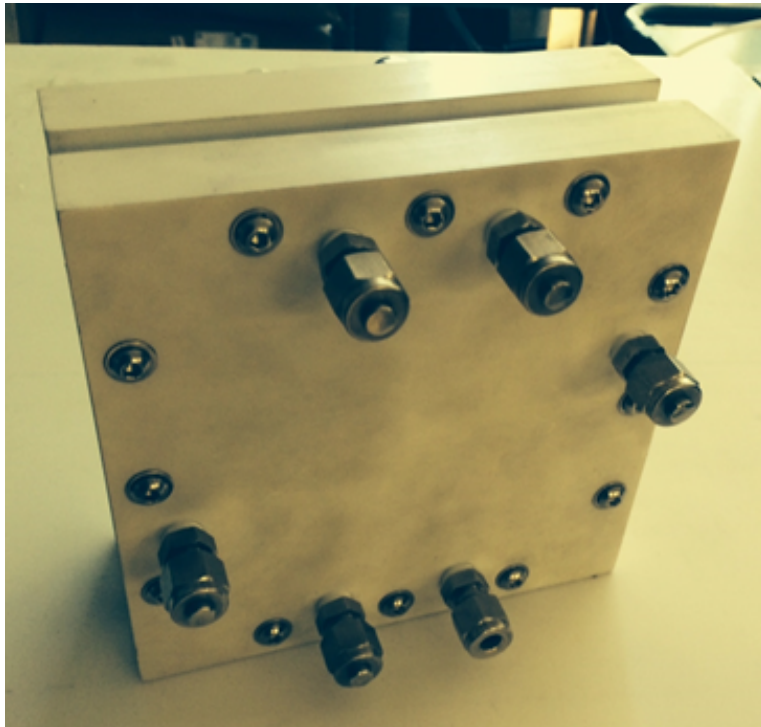


Figure A28.—Assembled Electrolysis Cell.

Appendix B.—Test Rig Design

B.1 Test Rig

Figure B1 shows the electrolysis cell test rig. Figure B2 shows a top view of the test rig. The test rig is built upon a four wheeled cart for easy movement into and out of a laboratory fume hood and easy relocation within the laboratory. The top of the wheeled cart is covered by an optical plate that was threaded with ¼-20 threaded holes for easy and flexible mounting of test rig components. The bottom shelf of the test rig contains the water bath.

Figure B3 shows the flow diagram for the test rig used for the impure water electrolysis testing. The impure water is stored in the holding tank and is pumped from the holding tank either through the electrolysis cell or through a bypass valve. The flow through the electrolysis cell was generally kept at 50 cc/min while the total flow through the holding tank was generally kept at 1000 cc/min. The pressure upstream and downstream of the electrolysis cell was kept at 2 to 4 psi to ensure that the cell water cavity was at a higher pressure than the electrolysis cell hydrogen cavity but not so high that the impure leaked out of the electrolysis cell water cavity into the hydrogen cavity.

The impure water exiting the electrolysis cell and the impure water flowing through the bypass valve flow through a coil of tubing immersed in a heated water bath which heats the impure water. The impure water then flows into the water holding tank. The holding tank is a clear walled plastic tank that has pad heaters attached to the outside of the holding tank to add more heat to the water. Early testing showed that the water was not getting to the desired temperature entering the electrolysis cell. The clear wall of the holding tank allowed the operator to monitor the water level during testing. The tubing and tube fitting were made of PVDF. The wettable surfaces of the test rig were deliberately made of non-metallic materials to minimize the possibility that the high ionic content of the water solution did not induce any corrosion, induce stray electrolysis reactions or impart any metallic ions into the water solution.

The water temperature in the holding tank, the temperature of the water entering the electrolysis cell, the temperature of the water exiting the electrolysis cell, and the temperature of the water bath were recorded on channels 1 through 4 of the data acquisition data logger. The pressure of the water entering and exiting the electrolysis cell were recorded on channels 5 and 6 of the data acquisition data logger. The electrolysis cell voltage and electrolysis current were recorded on channels 7 and 8 of the data acquisition data logger.

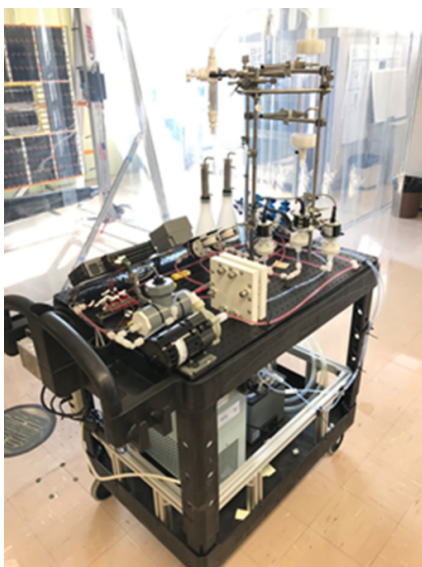


Figure B1.—Electrolysis Test Rig.

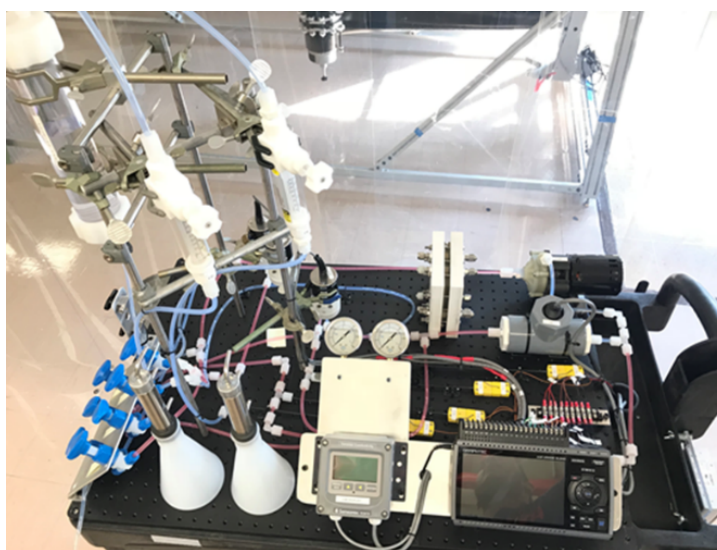


Figure B2.—Electrolysis Test Rig Top View.

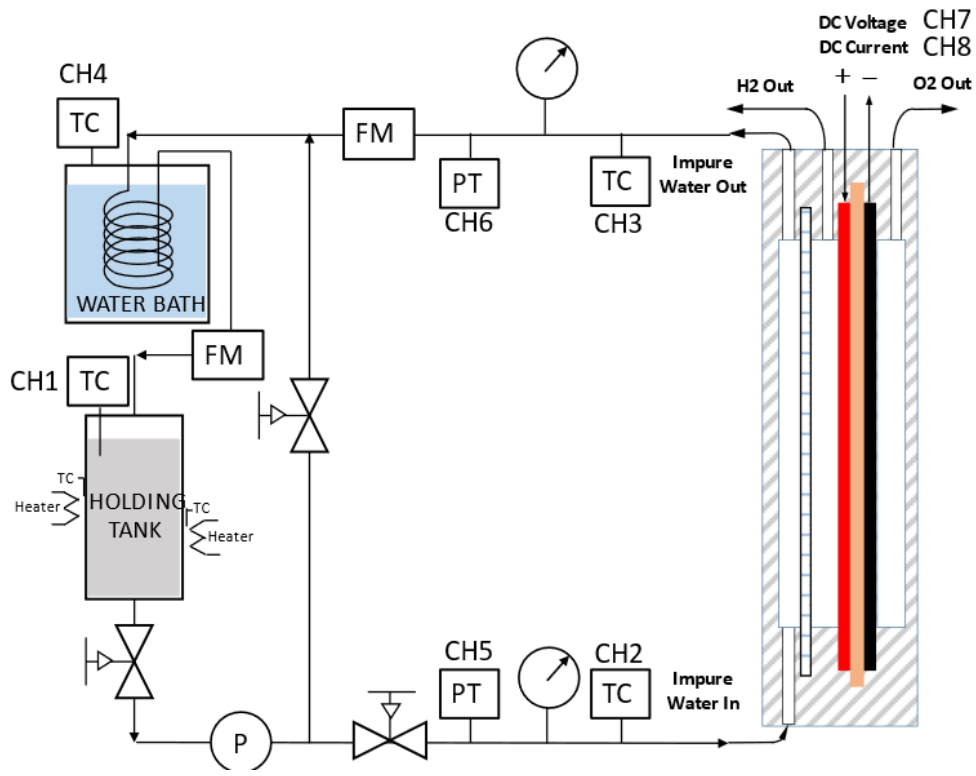


Figure B3.—Electrolysis Test Rig Flow Diagram.

B.2 Water Bath

The water bath shown in Figure B4 was a PolyScience water bath model WB-02. Table B1 lists the specifications for the water bath.



Figure B4.—Water Bath.

TABLE B1.—POLYSCIENCE WATER BATH MODEL WB-02 SPECIFICATIONS

Description	Gen. Purpose Water Bath, Digital
Display	Full-color TFT
Languages Supported	French, German, Spanish, Chinese, English
Reservoir Capacity (liters)	2
Reservoir/Tank Material	Stainless Steel
Reservoir Cover	Hinged Gable
Working Temperature Range °C	Ambient +5° to 100°
Temperature Stability °C	±0.1°
Maximum Ambient Temperature °C	40°
Temperature Calibration Capability	1-point
Working Access (L x W x D) (cm)	9.9 x 10.9 x 15.2
Flammability Class (DIN 12876-1)	I (NFL)
Over-Temperature Protection/Failsafe	Yes
Overall Dimensions (L x W x H) (cm)	30.5 x 22.9 x 34.3
Shipping Weight (kilograms)	4.1

B.3 Pump

The pump is a March Pump MDX model 0135-0174-0100. Series MDX are centrifugal magnetic drive pumps, eliminating the need for a shaft seal. Figure B5 shows the pump and Figure B6 shows the pump performance. The pump is not self-priming, lack a suction lift, and require a flooded suction. The pump cannot be run dry because the impeller requires the liquid being pumped for lubrication. The pump is plumbed on the suction side to the bottom of the water holding tank. Table B2 lists the specifications for the pump.



Figure B5.—Water Pump.

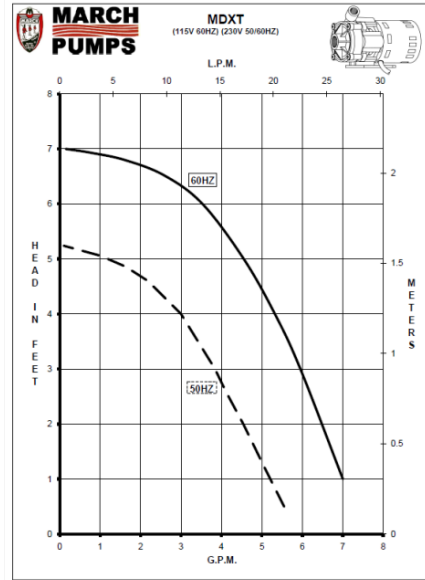


Figure B6.—Water Pump Performance.

TABLE B2.—MARK MODEL MXDT 0135-0174-0100 SPECIFICATION

Max Flow	(22LPM)
Max Head	(1.6M)
Inlet	1/2" OD 5/8" OD 1/2" FPT
Outlet	1/2" OD 5/8" OD 3/8" MPT
Pumping Power	1/55 hp
Pump Speed	1750 rpm
Electrical Power Voltage/Phase	115 or 230 VAC / 1 Phase
Electrical Power Current	0.94 A (115 VAC) / 0.45 A (230 VAC)
Motor Type	Air Cooled
Electrical Connection	Cord
Max Internal Pressure	50 PSI
Max Liquid Temperature	190F
Shipping Weight	5.5 lbs
Materials in Contact with Liquid	Polypropylene, Ceramic Shaft & Thrust Washer, Buna N, Ceramic Magnet
Size	7.75 x 4.88 x 3.88 L x H x W, inches

B.4 Holding Tank

Figure B7 shows the Holding Tank. The holding tank is a MilliporeSigma pressure vessel model MilliporeSigma™ XX1100000. The vertical mounting and the clear vessel body and the screw top endcap made it easy to monitor the water volume and refill the holding tank with water. The clear vessel body also made it easy to recognize that water flow had been established. Table B3 lists the specifications for the holding tank.



Figure B7.—Holding Tank Pump.

TABLE B3.—MILLIPORESIGMA XX1100000 SPECIFICATION

Description	Pressure Vessel
Type	Laboratory Filter Holders or Cyclones
Height (Metric)	41.9 cm
Inside Diameter	9 cm
Volume	600 mL
Material	Polycarbonate
Max. Pressure	6.9 bar
Autoclavable	Not Autoclavable
Sterility	Non-sterile

B.5 DC Power Supply

Figure B8 shows the Test Rig DC Power Supply Cart. Figures B9 and B10 show the front and back panels of the DC Power Supply. The DC Power Supply is a Volteq model HY1530EX which is a regulated variable switching DC power supply. Table B4 lists the specifications for the DC Power Supply. Ten of these units were mounted onto a single movable cart that provided an outlet strip to plug the power supplies into and a terminal strip that the outputs of the power supplies were wired to.



Figure B9.—Test Rig DC Power Supply Cart.



Figure B8.—DC Power Supply Front Panel.



Figure B10.—DC Power Supply Back Panel.

TABLE B4.—VOLTEQ MODEL HY1530EX SPECIFICATION

Description	Regulated variable switching DC power supply
Outputs	0-15 VDC and 0-30 A
Voltage Output Control	coarse and fine control knob
Current Output Control	coarse and fine control knob
Protection	over-voltage and reverse-voltage protection
Voltage Stabilization	$\leq 0.2\%$
Current Stabilization	$\leq 0.5\%$
Load Regulation	$\leq 0.3\%$
Ripple noise	CV $\leq 1\%$
LCD reading accuracy	$\pm 1\%$ ± 1 digit
Environment	0-40C, relative humidity $< 90\%$
Size	12" x 10" x 6"
Weight	12 lbs

B.6 Test Rig Data Acquisition

Figure B11 shows the Test Rig Data Logger used for data acquisition. The data acquisition uses a Graphtec Model GL840 Data Logger. The data logger was mounted onto the optical plate that was on top of the test rig cart. Nine data channels were used, 5 temperatures, 2 pressures, 1 current, and 1 voltage. The data was recorded onto a micro SD memory card that was inserted into the data logger. The data was recorded at a rate of once every 5 sec. Table B5 lists the specifications for the Test Rig Data Acquisition.



Figure B11.—Test Rig Data Logger.

TABLE B5.—GHRAPTEC MODEL GL840 DATA LOGGER SPECIFICATION

Description	Data acquisition data logger
Data Channel Inputs	20 Analog Signal Input Channels
Analog Input Terminals	Type: Multi-Input Type
Filter	Off, 2, 5, 10, 20, 40 (Moving Average in Selected Number)
Input Method	All channels Isolated Balanced Input, Scans channels for sampling
Type of Input Terminal	Screw Terminal (M3 Screw)
Digital Sensor	1 port for GL Digital Sensor
External Inputs	Trigger or Sampling (1 Channel); Logic/Pulse (4 Channels)
External Outputs	Alarm (4 Channels)
Input Voltage (Max)	Channels (-)/(-): 60 Vp-p, Channel / GND: 60 Vp-p
Max Voltage (Withstand \leq 1 min.)	Between Channels: 350 Vp-p, Channel / GND: 350 Vp-p
Measurement Ranges	Volts: 20, 50, 100, 200, 500mV; 1, 2, 5, 10, 20, 50V; 1 to 5 FS
	Thermocouple: Type K, J, E, T, R, S, B, N and W Supported
	RTD: PT100, JPT100, PT1000
	Humidity: 0 to 100% (w/ Graphtec B-530 Humidity Sensor)
Measurement Accuracy	Voltage: \pm 0.1% Full Scale
	Type K Thermocouple:
	• $-200^{\circ}\text{C} \leq \text{TS} \leq -100^{\circ}\text{C}$: $\pm(0.05\%$ of Rdg + 2.0°C)
	• $-100^{\circ}\text{C} < \text{TS} \leq 1370^{\circ}\text{C}$: $\pm(0.05\%$ of Rdg + 1.0°C)
Sampling Interval	Voltage: 10ms (1 Channel), 20ms (2 Channels), 50ms (5 Channels), 100ms (10 Channels) 200ms-1 Hour (All Channels)
	Temperature: 100ms (10 Channels) 200ms-1 Hour(All Channels)
Waveform Display Time Scale	1 second to 24 Hour/Division
Trigger, Alarm Function	OR or AND Condition at Level of Signal or Edge of Signal
	Start or Stop Capturing Data by the Trigger
	Alarm Condition: Rising, Falling, Window-in, Window-out
	Outputs a Signal When Alarm Occurs in the Input Signal
Interface to PC	Ethernet (10 Base-T/100 Base-Tx), USB (Hi-Speed)
Storage Capacity	Internal Storage: 4GB
	Media: SD Memory Card (SDHC up to 32GB)
Scaling Engineering Unit	Analog Voltage: Converts using Gain & Offset
	Temperature: Converts using 2 Reference Points
Display	Size: 7.0" TFT Color LCD (WVGA: 800 x 480 pixels)
Power Source	AC Adapter: 100 to 240 Volts AC, 50/60 Hz
	DC Power: 8.5 to 24 Volts DC,
Weight	1010 grams (35.63 ounces)
Dimensions	240mm x 158mm x 52.5mm (Excluding Protrusions)

Appendix C.—Test Results

C.1 Cell Testing Data—March 27, 2019

The testing on 03/27/19 was the first testing done with alkaline water electrolysis cell designed for use with contaminated water. This testing was done using deionized water to establish basic operating performance prior to testing with any contaminated water source. This testing also helped to identify aspects of the test rig design or operation that might need improvement for future testing. The cell used the Sustainion[®] 37 to 50 membrane manufactured by Dioxide Materials (Ref. 1). Data comparing the Sustainion[®] 37 to 50 membrane to other membranes is shown in Figure C1 and Table C1.

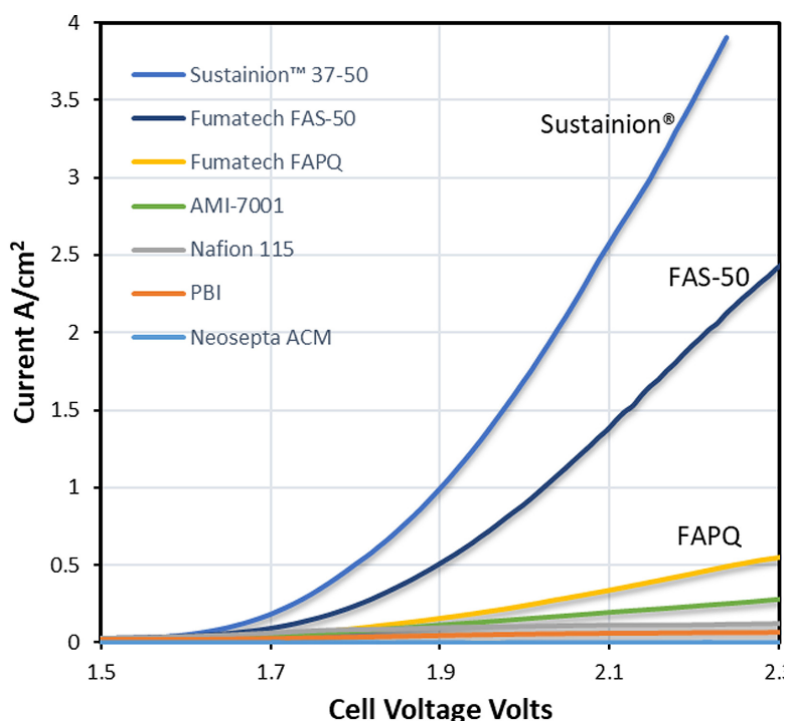


Figure C1.—Linear sweep voltammogram taken with an alkaline water electrolyzer with a FeNiO₄ anode catalyst and a FeNiCo cathode catalyst in 1M KOH at 60 °C.

TABLE C1.—THE ASR MEASURED FOR SEVERAL MEMBRANES AT 60 °C IN 1M KOH (REF. 1)

Membrane	Sustainion [®] 37-50	FAS-50	Nafion 115	FAPQ	AMI-7001	PBI	ACM
Thickness	50 μm	50 μm	125 μm	75 μm	450 μm	50 μm	110 μm
ASR Ω-cm ²	0.045	0.3783	0.52	0.83	2.0	8.3	>50

C.1.2 Test Objectives

The key questions to be answered in this first test were:

- 1) Was there enough heat from the water bath to heat the water in the holding tank and through the electrolysis cell to get the electrolysis cell to an acceptable level (50°C cell temperature)?
- 2) Was there going to be a sufficient water flow through the electrolysis cell without over pressurizing the water cavity within the cell?

The membrane was tested for leakage by pressurizing the water cavity to 5 psid (max), and observing whether any liquid water leaked around or through the porous Teflon membrane.

- 3) Would the electrolysis cell polarize and produce hydrogen and oxygen in quantities consistent with the electrical current flowing through the electrolysis cell?
- 4) Would there be enough water distilling from the electrolysis cell water cavity to meet the water use at both the electrodes, and prevent the electrolysis cell from drying out?

The higher the temperature of the water within the cell the higher the water distillation rate would be and therefore the higher the current can be.

- 5) What magnitude of electrical current could the electrolysis cell stably operate?
- 6) What voltage would the electrolysis operate relative to the electrical current?

C.1.3 Results

Figure C2 shows the water bath temperature, holding tank temperature, and difference in temperature between the water bath and the holding tank versus elapsed time. The water bath temperature setpoint was initially set to 70 °C. After about 2 hr the setpoint was raised to 75 °C. The water bath never reached either setpoint, indicating that there was insufficient heating to overcome heat losses as water was circulated through the holding tank and electrolysis cell. Figure C2 also shows the difference in temperature between the water bath and the holding tank versus elapsed time. The difference reached a steady state of about 15 °C. Future testing would require additional heating of the circulating water in order to raise the temperature within the holding tank to higher than 50 °C.

The water flow through the water bath and holding tank was approximately 750 to 800 cc/min. The water flow through the electrolysis cell was approximately 25 cc/min. Assuming no waste heat was absorbed and dissipated by the cell's surrounding structure, at 25 cc/min, the water should increase in temperature by 0.57 °C per watt of absorbed waste heat from the electrolysis cell. Since the testing was done with a single cell which had two cell endplates, and that the waste heat generated by the electrolysis cell was likely to be less than 10 watts, 25 cc/min was considered adequate. At 1-1/2 hr into the test the water flow through the electrolysis cell was increased from 25 to 50 cc/min. The water pressure immediately upstream of the electrolysis cell was 3.00 psi and immediately downstream was 2.87 psi. The 0.13 psi pressure drop was acceptable, and the 3 psi water cavity pressure was within the 5 psi acceptance water cavity pressure. During the testing no water was observed leaking out of the cell or into the cell's hydrogen or oxygen cavities.

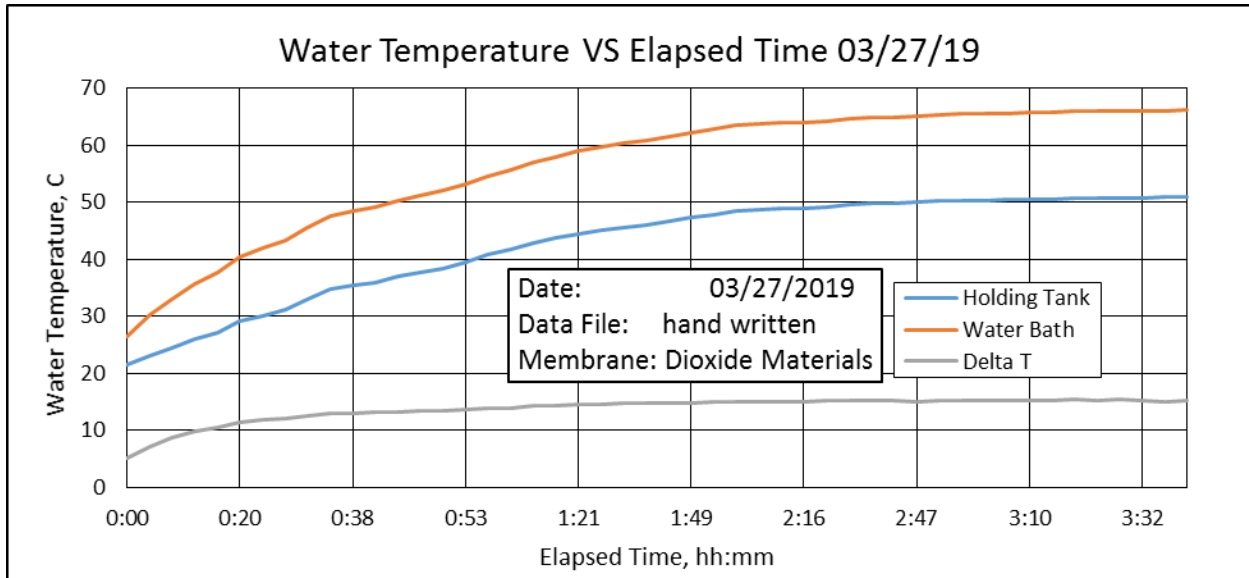


Figure C2.—Water Temperature vs. Elapsed Time 03/27/2019.

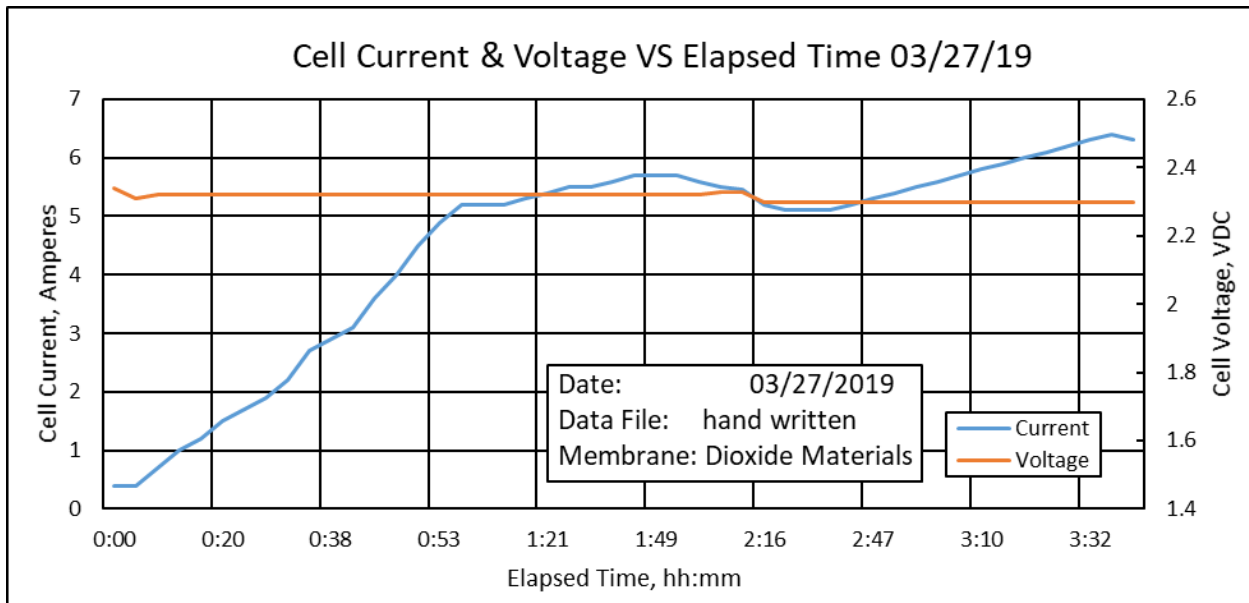


Figure C3.—Cell Current & Voltage vs. Elapsed Time 03/27/2019.

Figure C3 shows the cell current and cell voltage versus elapsed time. As the temperature of the water flowing through the electrolysis increased the electrical current was adjusted upward. Increasing the temperature of the water flowing through the electrolysis cell increases the vapor pressure of the water which increases the vapor pressure gradient that exists between the water in the cell's water cavity and the water vapor pressure at the cathode electrode's surface. The increased water vapor pressure gradient causes water vapor to be transported to the cathode electrode at a faster rate which allows the cell to electrolyze water at a faster rate without drying the cell out. The cell voltage was observed and interpreted as an indicator of general cell health and in particular, the cell's level of hydration. An increasing cell voltage would be a sign of the cell drying out. If the cell dries out too much there is a greater opportunity for hydrogen and oxygen to come in contact with each other through the cell ion exchange separator. Figure C3 shows the cell current was adjusted from 0.4 to 5.7 A during the first 2 hr of the testing.

TABLE C2.—ANODE (OXYGEN) SIDE

Cell Current Amperes	Cell Current Density mA/cm ²	Calculated Water Use ml/min	Calculated Oxygen Flow gms/min	Calculated Oxygen Flow cm ³ /min	Calculated Anode Total Flow cm ³ /min	Calculated Time to flow 25cc seconds	Measured Time to flow 25cc seconds	Estimated Current Efficiency %
5.2	52	0.029	0.03	20.42	21.08	71.17	70.55	100.88
5.6	56	0.031	0.03	22.28	23.00	65.21	66.22	98.48
5.7	57	0.032	0.03	22.68	23.41	64.07	64.52	99.30

TABLE C3.—CATHODE (HYDROGEN) SIDE

Cell Current Amperes	Cell Current Density mA/cm ²	Calculated Water Use ml/min	Calculated Hydrogen Flow gms/min	Calculated Hydrogen Flow cm ³ /min	Calculated Cathode Total Flow cm ³ /min	Calculated Time to flow 25cc seconds	Measured Time to flow 25cc seconds	Estimated Current Efficiency %
5.2	52	0.029	0.003	41.38	42.72	35.11	36.00	97.54
5.3	53	0.030	0.003	42.18	43.54	34.45	35.81	96.21
5.4	54	0.030	0.003	42.97	44.36	33.81	35.07	96.42
5.5	55	0.031	0.003	43.77	45.18	33.20	34.36	96.62

During this first 2 hr the cell voltage stayed constant at about 2.3 V which indicated stable operation. Over the remaining 1 hr to 50 min, the current was gradually increased from 5.2 to 6.3 A, and the cell voltage continued to remain at about 2.3 V.

Another important aspect to this testing was to measure the rate of hydrogen and oxygen gas evolution and compare it to a calculated theoretical rate based on the cell current. Oxygen and hydrogen gas flow rates were measured using a gas bubble flow meter. The time needed for either gas to push a gas bubble film through a 25cc volume glass tube was measured and the rate then calculated. Tables C2 and C3 list the gas flow measurements taken at the corresponding electrical currents and compares the measured flow rates with the theoretical rates. An electrical current efficiency which is the fraction of the measured rate divided by the calculated rate was then calculated. Table C2 shows that the actual oxygen generation was 99.6±1.2%. Sources of error in this measurement include inaccuracy in the electrical current measurement and the time measurement. Table C3 shows that the actual hydrogen generation was 96.9±0.65%. The consistently lower hydrogen current efficiency could be due to measurement inaccuracy as well, but also some hydrogen might be dissolving in the water flowing through the water cavity. Another possible hydrogen loss could be from oxygen dissolved in the water flowing through the water cavity recombining with hydrogen in the hydrogen cavity. The hydrogen current efficiency is still close to 100%.

The testing on March 27, 2019 was completed without incident after nearly 4 hr of operation.

C.1.3 Conclusions

The test rig heated the water in the holding tank to about 50 °C. The water distilled from the cell's water cavity cell's hydrogen electrode at a rate that allowed the cell to operate at up to 6.3 A during this test. The pressure of the water inside the cell's water cavity was less than 3 psi which kept liquid water from leaking out of the cell's water cavity.

The oxygen and hydrogen flow rates leaving the cell were measured and compared to the theoretical flow rates based on the electrical current. The calculated total flow rates account for both the gas flow and the water vapor flow that comes out with the gas. The time to fill a 25cc soap bubble flow meter was calculated. The actual time to fill a 25cc soap bubble flow meter that was measured. The oxygen/water vapor flow rate measured was 98.48 to 100.88% of the expected flow. This result was interpreted as 100% current efficiency based on the margin of error and precision of the measurement. The

hydrogen/water vapor flow rate measured was 96.2 to 97.5% of the expected flow. Some of the hydrogen was expected to leave the cell dissolved in the water circulated through the cell's water cavity, and some of the oxygen dissolved in the water might be recombining with the hydrogen inside the cell.

The cell operation was stable. Water droplets exiting the cell with the gas were not observed, indicating that the water distilling from the water cavity was not condensing and collecting in the hydrogen cavity. The cell showed no signs of being dried out by electrolysis since the cell voltage was stable.

C.2 Cell Testing Data—March 28, 2019

Prior to the start of the testing on March 28, several changes to the test rig were installed. A SD memory card was installed into the Graphtec GL840 Data Logger so that data logged could be stored and processed off line after the conclusion of the test. This was the case for all subsequent tests. Thermocouples were installed in the water line connections to the electrolysis cell immediately upstream and immediately downstream of the cell, and the data recorded by the Graphtec data Logger on Channel 2 and Channel 3, respectively. The average of these two temperatures was taken as the estimate of the electrolysis cell temperature. In general, the downstream temperature was higher by between 0.3 and 1 °C.

C.2.1 Results

Figure C4 shows the water bath temperature, holding tank temperature, and difference in temperature between the water bath and the holding tank versus elapsed time, and the cell water temperature. The water bath temperature setpoint was set to 75 °C. The recirculation between the water bath and the holding tank was adjusted to approximately 1000 cc/min, and the water flow through the electrolysis cell was adjusted to 50 cc/min. The water bath never reached the 75 °C setpoint, and Figure C4 also shows the difference in temperature between the water bath and the holding tank reached a steady state of about 11 °C. The cell temperature was consistently lower than the holding tank, indicating heat loss in water line prior to entering the cell.

Figure C5 shows the cell current and cell voltage versus elapsed time. The cell voltage was adjusted stepwise (1.9 VDC at the start of the test, then 2.15 VDC, 2.28 VDC, and finally approximately 2.35 VDC where it was kept through the balance of the test). Figure C5 shows the cell current increased over the duration of the test. The current at the end of the test was 1.8 A while the cell voltage was 2.35 VDC. This electrochemical performance was poorer than observed on March 27 where at 2.3 VDC the cell current was greater than 5 A.

After this test it was noticed that the endplate on the cathode side of the cell had developed a crack. This endplate was replaced, and the cell reassembled, but before testing resumed the endplate on the anode side of the cell severely cracked (Figure C6). Table C4 shows the polyester material used for the endplates had a low impact strength rating. New endplates were fabricated using polycarbonate and 20% glass filled polycarbonate both of which had a better impact strength rating which reduces the likelihood of cracking.

Four sets of endplates were ordered as replacements for the polyester endplates that exhibited fractures. Of the four sets of endplates remade, one set was made of polycarbonate using the same one inch thickness. Another set was also made of polycarbonate, 1-1/2 in. thickness to compensate for the reduced tensile strength compared to the polyester. Two sets (1 in. thickness) were made of a 20% glass-filled polycarbonate that showed both higher impact strength and higher tensile strength than the polyester.

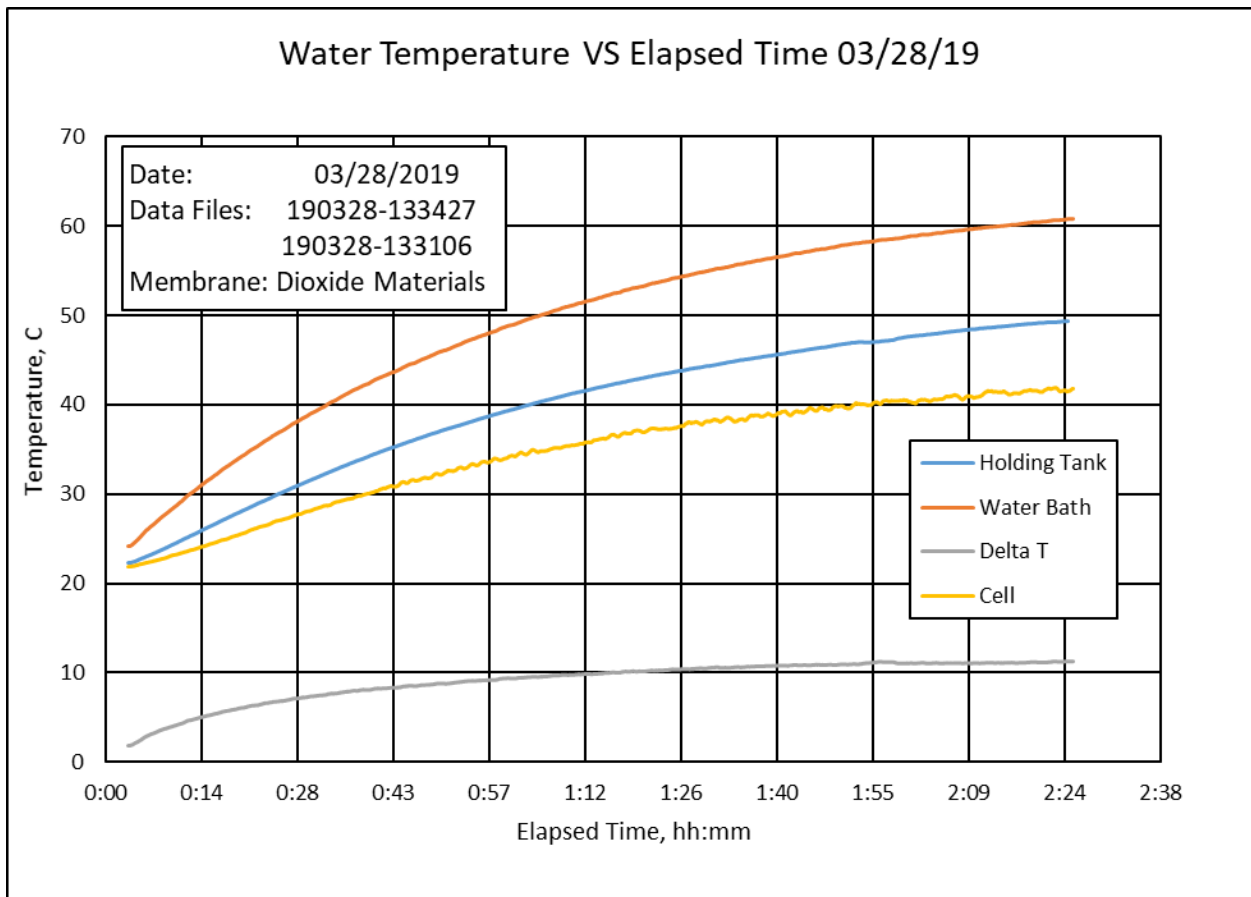


Figure C4.—Water Temperature vs Elapsed Time 03/28/2019.

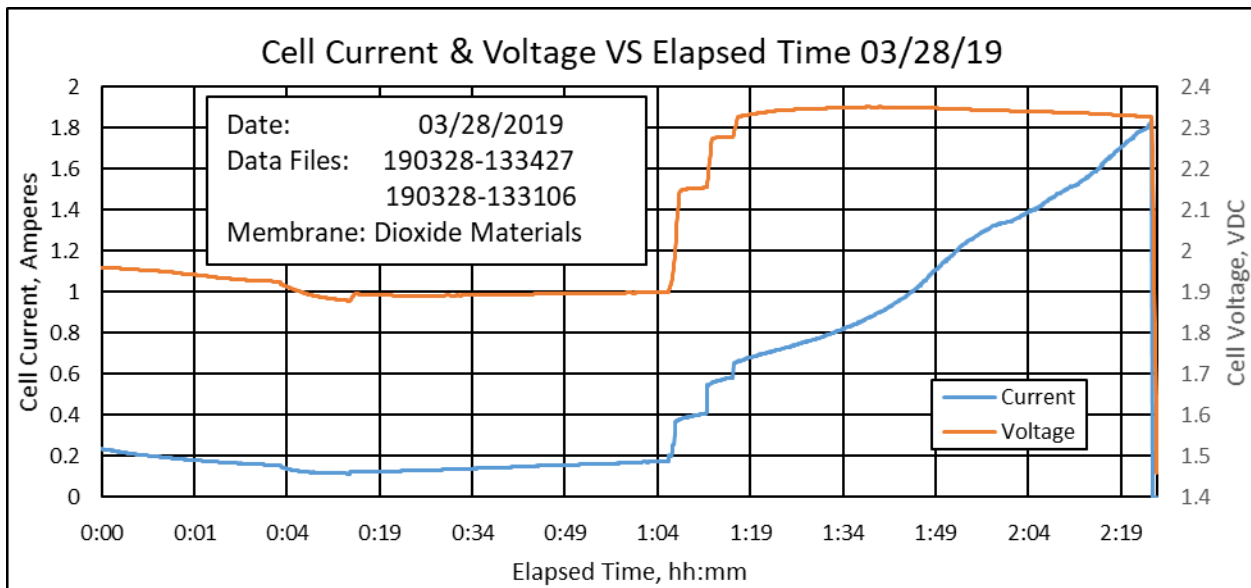


Figure C5.—Cell Current & Voltage vs Elapsed Time 03/28/2019.

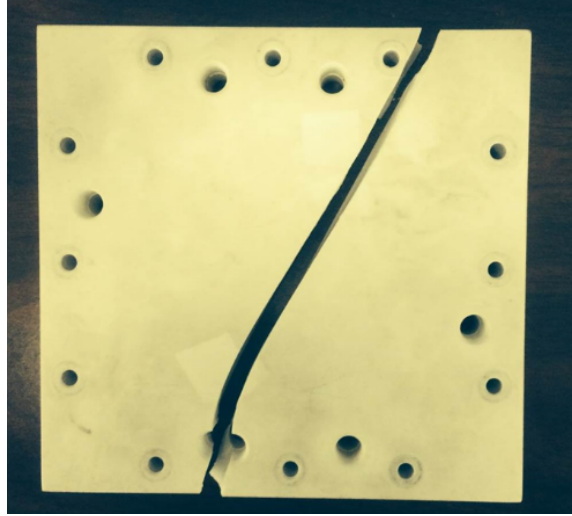


Figure C6.—Cracked Polyester Cell Endplate 03/28/2019.

TABLE C4.—MATERIAL PROPERTIES OF ELECTROLYZER ENDPLATE MATERIALS

Material	Polyester Plastic	Polycarbonate Plastic	Polycarbonate Plastic 20% Glass Filled
Impact Strength	0.65 ft.-lbs./in.	2 ft.-lbs./in.	2.06 ft.-lbs./in.
Impact Strength Rating	Poor	Good	Good
Tensile Strength	11,600 psi	9,100-9,500 psi	12,000 psi
Tensile Strength Rating	Good	Good	Excellent

C.3 Cell Testing Data—July 17, 2019

Prior to the start of the testing on July 17 new replacement endplates were fabricated. The cell was rebuilt initially with the 1 inch thick polycarbonate endplates, but during the assembly process one of the endplates developed a hairline crack. This crack was revealed during the pressure integrity test of the rebuilt cell prior to electrolysis testing. The cell was rebuilt a second time with one of the sets of 20% glass-filled endplates, and the cell passed the pressure integrity test. One of the 20% glass-filled polycarbonate endplates is shown below (Figure C7). The cell was mounted on the test rig and was tested for electrolysis performance.

C.3.1 Results

Figure C8 shows the water bath temperature, holding tank temperature, and difference in temperature between the water bath and the holding tank versus elapsed time, and the cell water temperature. The water bath temperature setpoint was set to 75 °C. The recirculation between the water bath and the holding tank was adjusted to approximately 1000 cc/min, and the water flow through the electrolysis cell was adjusted to 50 cc/min. The water bath reached the 51 °C during the 50 min of testing. The holding tank reached 43 °C during the test. Figure C8 also shows the difference in temperature between the water bath and the holding tank reached 7.7 °C. The cell temperature reached 36.6 °C during the test.

Figure C9 shows the cell current and voltage versus elapsed time. The cell operated at a voltage of 1.87 to 1.88 VDC. The current was increased while the cell voltage between 1.87 to 1.88 VDC range. As the cell temperature increased to 36.6 °C the cell was able to tolerate higher current.



Figure C7.—The 20% Glass-Filled Polycarbonate Endplate.

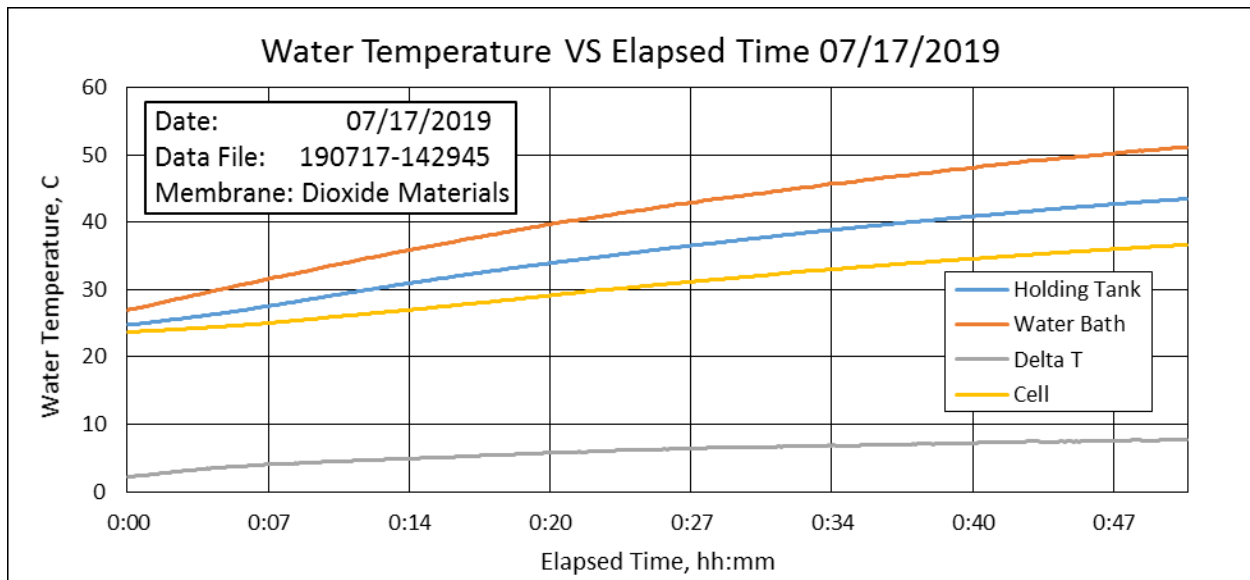


Figure C8.—Water Temperature vs. Elapsed Time 07/17/2019.

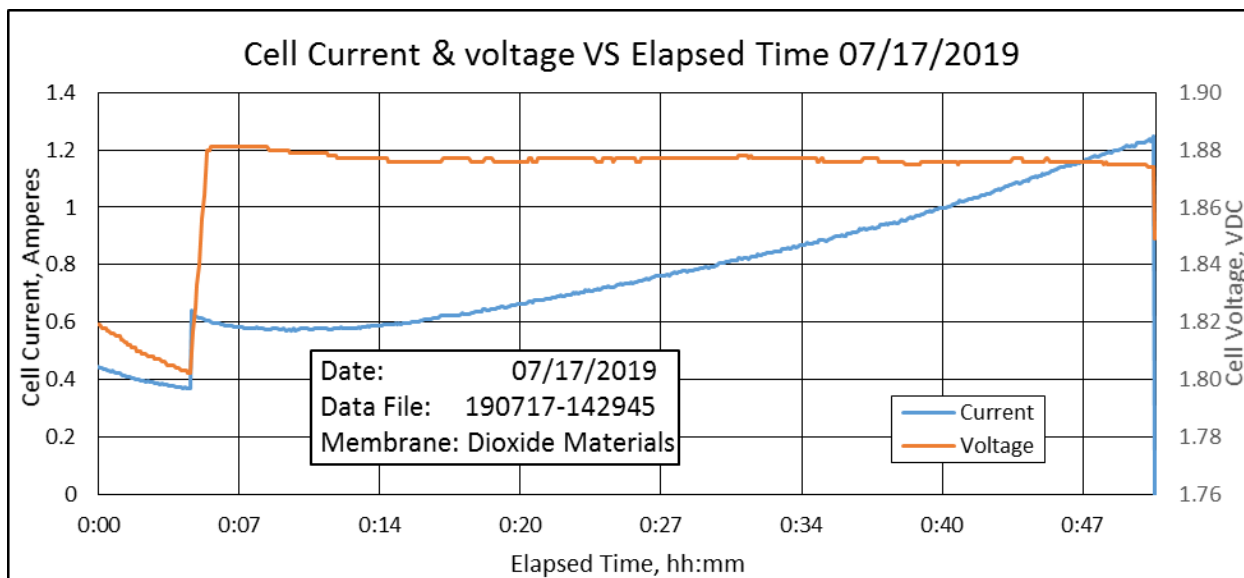


Figure C9.—Cell Current & Voltage vs Elapsed Time 07/17/2019.

C.4 Cell Testing Data—July 18, 2019

The testing on July 18 lasted a little over 3 hr which allowed the cell to get to a higher temperature than the testing on July 17. The temperature difference between the water bath and the holding tank steadied out at slightly less than 10 °C even though the temperature of both the water bath and holding tank continued to climb during the test.

C.4.1 Results

Figure C10 shows the water bath temperature, holding tank temperature, and difference in temperature between the water bath and the holding tank versus elapsed time, and the cell water temperature. The water bath temperature setpoint was set to 75 °C. The recirculation between the water bath and the holding tank was adjusted to approximately 1000 cc/min, and the water flow through the electrolysis cell was adjusted to 50 cc/min. The water bath reached the 63.3 °C during the 3 hr of testing. The holding tank reached 54.5 °C during the test. Figure C10 also shows the difference in temperature between the water bath and the holding tank reached 8.8 °C. The cell temperature reached 47.8 °C during the test.

Figure C11 shows the cell current and cell voltage versus elapsed time. The cell current was adjusted to about 0.6 A, but the cell voltage started to climb which was a possible indication of cell dryout. The current was decreased to about 0.5 A. As the voltage continued to climb the current was lowered, eventually to 0.3 A to allow the cell performance to stabilize. The cell stabilized at a voltage of 1.89 VDC and a cell current of about 0.45 A. As the cell warmed up and rehydrated the current was gradually increased, maintain a cell voltage of 1.88 to 1.89 VDC. This approach continued until 2 hr and 15 min into the test, at which point the cell current was about 3.6 A at a cell voltage of 1.91 VDC. The current was then raised to 5.5 A and a voltage of 1.94 VDC eventually stabilizing at 1.99 VDC. At 2 hr and 20 min, with the current at 5.53 A the hydrogen flow exiting the cell was measured with a soap bubble flowmeter. The hydrogen flow was again measured at 2 hr and 21 min, with the current at 5.56 A, and still again at 2 hr 22 min with the current at 5.6 A.

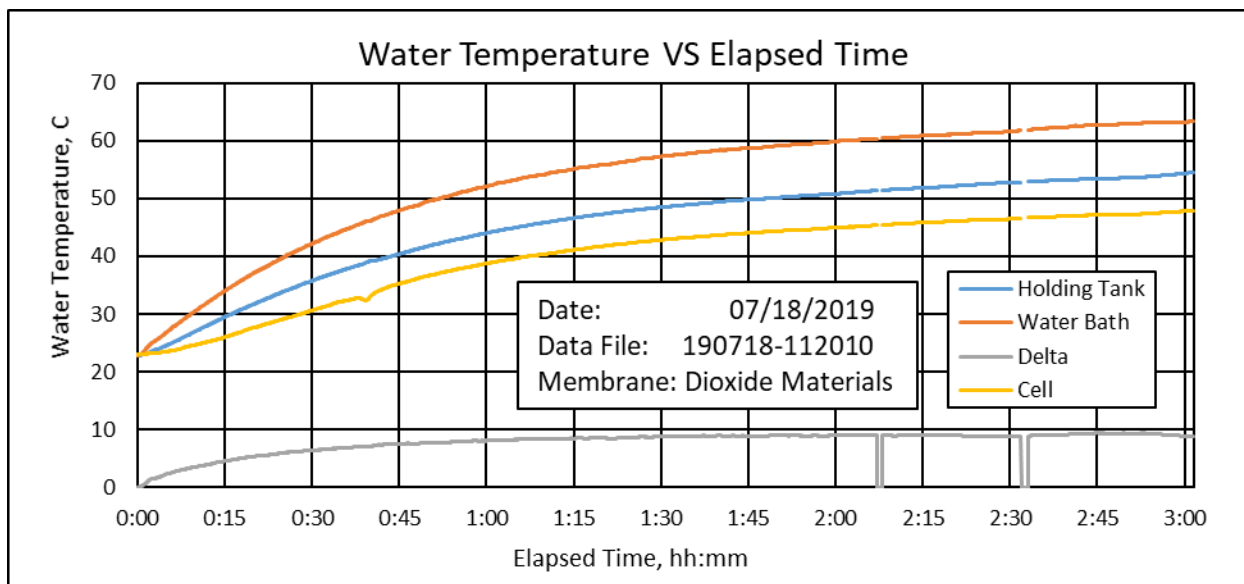


Figure C10.—Water Temperature vs Elapsed Time 07/18/2019.

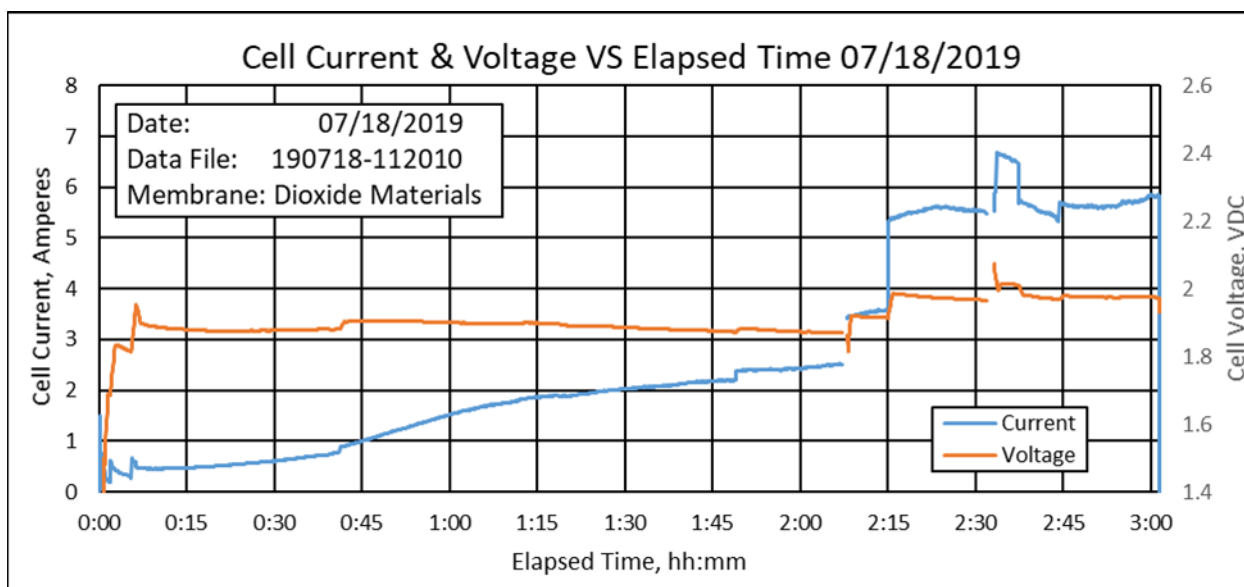


Figure C11.—Cell Current & Voltage vs. Elapsed Time 07/18/2019.

At 2 hr 24 min the oxygen flow exiting the cell at 5.612 A was measured with a soap bubble flowmeter. The oxygen flow was again measured at 2 hr 27 min, with the current at 5.54 A, and still again at 2 hr 28 min with the current at 5.55 A. The measured gas flow rates are compared against the theoretical flow rates in Table C5. At 2 hr and 33 min the cell current was increased to 6.6 A and the cell voltage increased to 2.01 VDC. At 2 hr and 37 min the current was returned to 5.6 A and kept at about that level for the balance of the test.

The hydrogen flow measurements were slightly lower than would theoretically be expected, while the oxygen flows were essentially exactly as expected. This was a similar result as was obtained March 27.

TABLE C5.—ANODE (OXYGEN) SIDE AND CATHODE (HYDROGEN) SIDE

Anode (Oxygen) Side								
Cell	Cell	Water	Oxygen	Oxygen	Total Anode	Calculated	Measured	Estimated
Current	Current Density	Consumption	Flow	Flow	Flow	Time to	Time to	Current
Amperes	mA/cm ²	ml/min	gms/min	cm ³ /min	cm ³ /min	flow 25cc	flow 25cc	Efficiency
						seconds	seconds	%
5.612	56.12	0.031	0.028	22.33	23.05	65.07	65.15	99.88
5.54	55.4	0.031	0.028	22.04	22.76	65.92	65.7	100.33
5.555	55.55	0.031	0.028	22.10	22.82	65.74	65.62	100.18
Cathode (Hydrogen) Side								
Cell	Cell	Water	Hydrogen	Hydrogen	Total Cathode	Calculated	Measured	Estimated
Current	Current Density	Consumption	Flow	Flow	Flow	Time to	Time to	Current
Amperes	mA/cm ²	ml/min	gms/min	cm ³ /min	cm ³ /min	flow 25cc	flow 25cc	Efficiency
						seconds	seconds	%
5.53	55.3	0.031	0.003	44.01	45.43	33.02	36.00	91.72
5.56	55.6	0.031	0.003	44.24	45.67	32.84	34.44	95.36
5.602	56.02	0.031	0.003	44.58	46.02	32.59	34.40	94.75
Ambient Laboratory Environment 25C; 1.0 atm					Cell Temperature 40C			

C.5 Cell Testing Data—July 23, 2019

Prior to the start of testing the test rig had been modified to allow the cell to be tested at higher temperatures. A heater was added to the outside of the holding tank to add additional heat to the circulating water.

The testing on July 23 lasted a little 3 hr and 32 min. The added heater allowed the cell to get to 51.7 °C during the test versus 47.8 °C on July 18. The temperature difference between the water bath and the holding tank steadied out at slightly less than 10.8 °C even though the temperature of both the water bath and holding tank continued to climb during the test.

C.5.1 Results

Figure C12 shows the water bath temperature, holding tank temperature, and difference in temperature between the water bath and the holding tank versus elapsed time, and the cell water temperature. The water bath temperature setpoint was set to 75 °C. The recirculation between the water bath and the holding tank was adjusted to approximately 1000 cc/min, and the water flow through the electrolysis cell was adjusted to 50 cc/min. The water bath reached 67.9 °C during the 3 hr and 32 min of testing. The holding tank reached 57 °C during the test. Figure C12 also shows the difference in temperature between the water bath and the holding tank reached 10.8 °C. The cell temperature reached 51.7 °C during the test, so the heater was successful at increasing the cell temperature during testing, though not as much as was desired.

Figure C13 shows the cell current and cell voltage versus elapsed time. The cell current was initially adjusted to about 0.6 A with a cell voltage of 1.83 VDC, but the cell voltage started to climb which was a possible indication of cell dryout. The current was lowered, eventually to 0.3 A with a cell voltage of 1.78 VDC. At 5 min into the test, the cell current was increased to 0.4 A and a cell voltage of 1.87 VDC. At about 19 min into the test the current was increased to 0.45 A and the cell voltage went up to 1.9 VDC. The current was gradually raised to 0.8 A over the next 30 min (52 min into the test), keeping the cell

voltage at approximately 1.9 VDC. At 52 min into the test the current was raised to about 1.0 A and the cell voltage went up to 1.96 VDC. Over the next 34 min (1 hr 26 min into the test) the current was gradually raised to 2.5 A, and the voltage went to 1.93 VDC. Over the next 1 hr 12 min (2 hr 38 min into the test) the current was increased stepwise to 7.0 A while keeping the cell voltage under 2.0 VDC. At 2 hr and 38 min into the test the current was raised to approximately 10 A and the cell voltage went up to about 2.1 VDC. The cell operated at 10 A for about 20 min and then the cell voltage started to climb indicating potential cell dryout. The current was reduced, but the cell voltage continued to go up. At about 3 hr 15 min into the test the current was reduced to 7.5 A, but the voltage continues to go up, and at 3 hr and 32 min into the test the test was stopped.

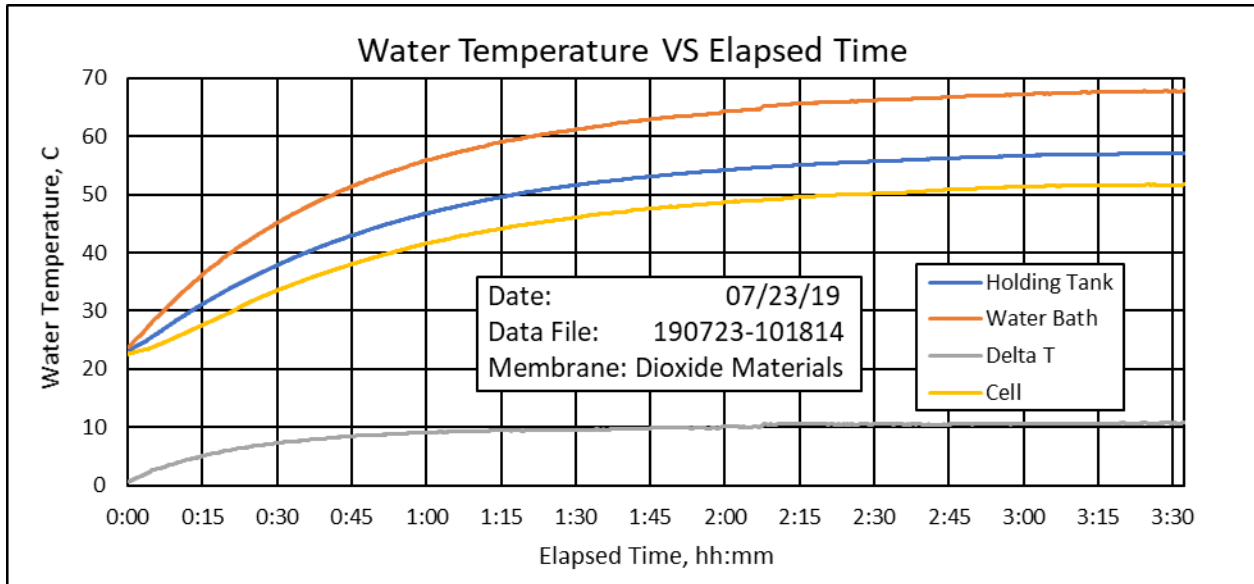


Figure C12.—Water Temperature vs. Elapsed Time 07/23/2019.

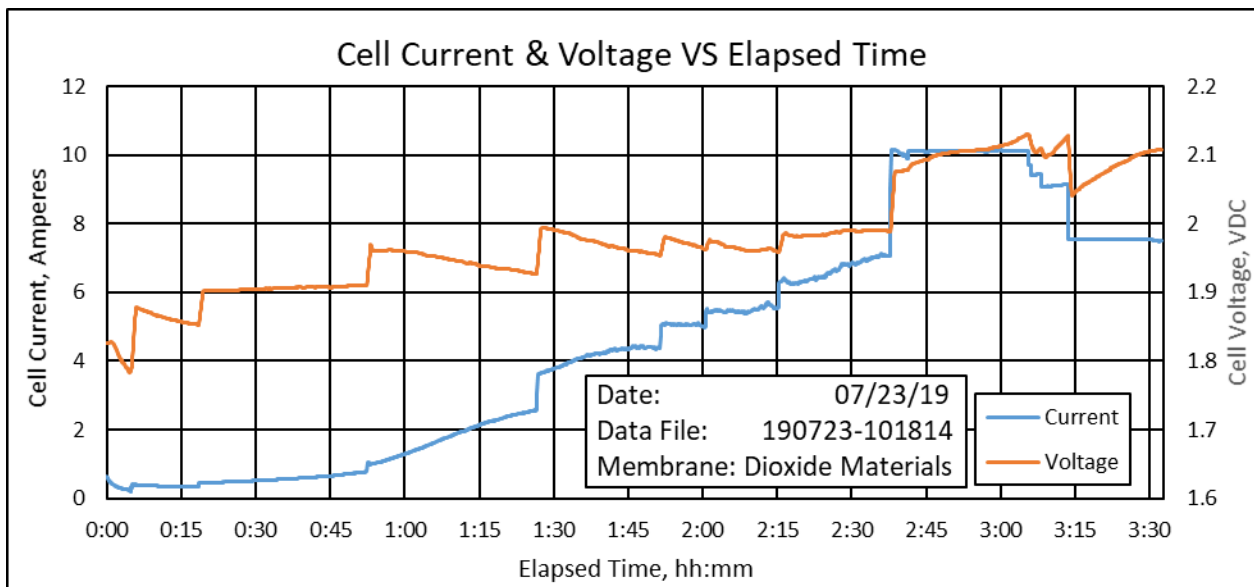


Figure C13.—Cell Current & Voltage vs. Elapsed Time 07/23/2019.

C.6 Cell Testing Data—July 26, 2019

The testing on July 26 lasted a little 2 hr and 27 min.

C.6.1 Results

Figure C14 shows the water bath temperature, holding tank temperature, and difference in temperature between the water bath and the holding tank versus elapsed time, and the cell water temperature. The water bath temperature setpoint was set to 75 °C. The recirculation between the water bath and the holding tank was adjusted to approximately 1000 cc/min, and the water flow through the electrolysis cell was adjusted to 50 cc/min. The cell was pre-heated to about 30 °C before current was applied to the cell. The water bath reached 68.3 °C during the 2 hr and 27 min of testing. The holding tank reached 57.2 °C during the test. Figure C14 also shows the difference in temperature between the water bath and the holding tank reached 11.0 °C. The cell temperature reached 51.6 °C during the test.

Figure C15 shows the cell current and cell voltage versus elapsed time. The cell current was initially adjusted to about 1.0 A with a cell voltage of 1.83 VDC. The cell current was gradually increased to 1.5 A over the first 26 min of the test while keeping the cell voltage at about 1.83 VDC. At 26 min into the test the cell current was increased to 2.0 A and the voltage rose to 1.87 VDC. The cell current remained at 2.0 A for the next 29 min (55 min into the test), the cell voltage stayed at 1.87 VDC. At 55 min into the test the current was raised to 3.2 A and the voltage went to 1.94 VDC eventually climbing to 1.97 VDC over the next 4 min. The current was reduced to 2.0 A over the next 9 min (1 hr 8 min into the test) and the cell voltage dropped to 1.87 VDC. The current remained at 2.0 A over the next 35 min, and during this time the cell voltage increased to 1.90 VDC. At 1 hr 43 min into the test the current was raised to 2.25 A and was periodically raised over the next 41 min until at 2 hr and 24 min the current reached 7.0 A and the cell voltage was 2.42 VDC. The current was reduced to 0 over the next 3 min, and the test was stopped at 2 hr 27 min of testing. After testing the cell was removed from the test rig and the cell oxygen cavity was flooded with 1M KOH to ensure the cell was rehydrated.

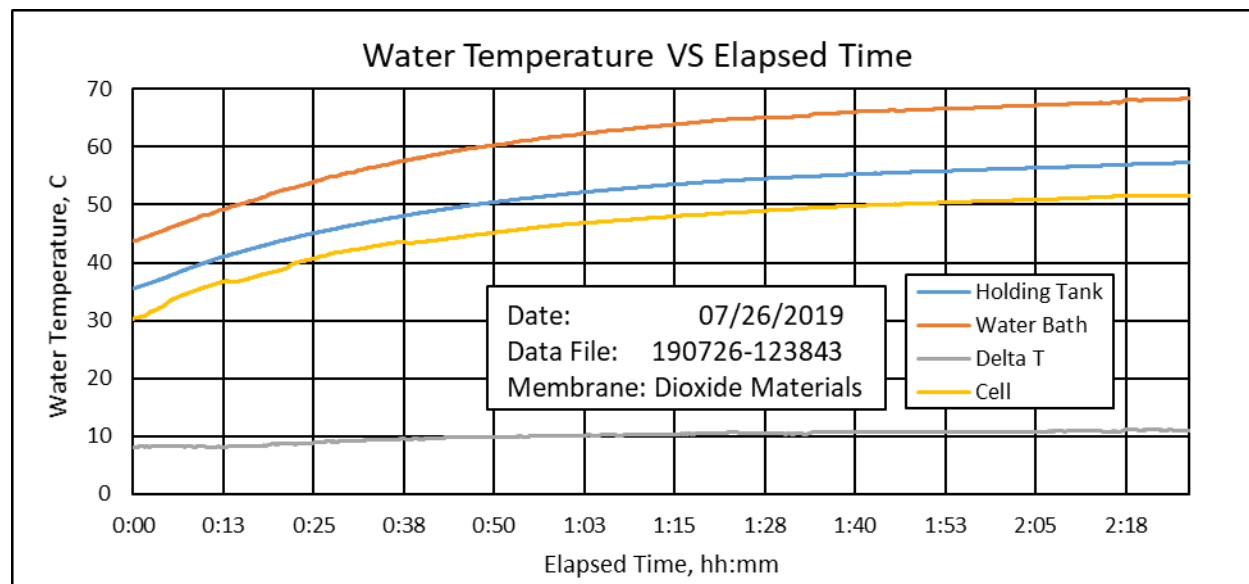


Figure C14.—Water Temperature vs. Elapsed Time 07/26/2019.

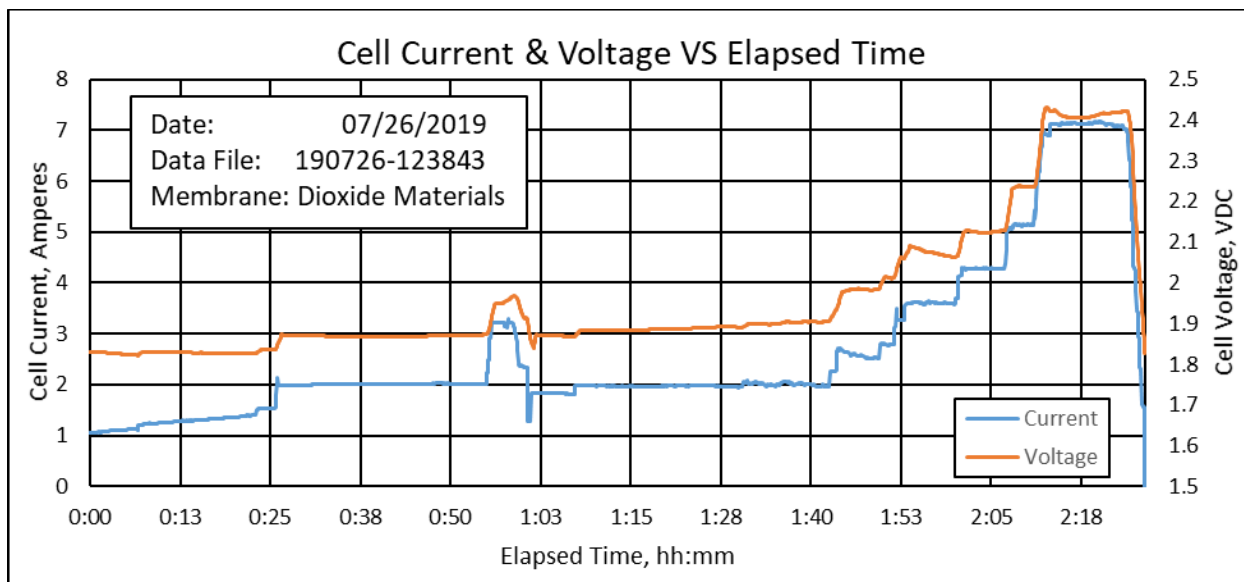


Figure C15.—Cell Current & Voltage vs. Elapsed Time 07/26/2019.

TABLE C7.—MARS ISRU WATER MIXTURE USED FOR TESTING

Reagent Name	Chemical Formula	Amount	Unit	Amount	Unit
Water	H ₂ O	25	ml	2000	ml
Calcium Carbonate	CaCO ₃	40	mg	3200	mg
Magnesium Carbonate	MgCO ₃	20	mg	1600	mg
Magnesium Sulfate Heptahydrate	MgSO ₄ * 7H ₂ O	30	mg	2400	mg
Potassium Chloride	KCl	0.8	mg	64	mg
Sodium Bicarbonate	NaHCO ₃	3	mg	240	mg
Calcium Chlorate Tetrahydrate	Ca(ClO ₄) ₂ *4H ₂ O	11.5	mg	920	mg
Magnesium Chlorate Hexahydrate	Mg(ClO ₄) ₂ *6H ₂ O	8.3	mg	664	mg

C.7 Cell Testing Data—July 30, 2019

A simulated Mars ISRU water mixture composition was used for testing on July 30, 2019. The Mars ISRU contaminated water mixture composition shown in Table C7 was provided by the NASA ISRU team. The two chlorates were not used (they were not available at the time the mixture was made). A 2 liter quantity was produced for the testing. The salts were added to 2000 ml of deionized water and stirred for 24 hr. The two carbonates did not completely dissolve. The mixture after stirring was milky white with the excess carbonate suspended in solution. The solution was filtered to remove the undissolved salt. The solution replaced the deionized water on the test rig previously used for testing.

The cell's oxygen cavity had been flooded with 1M KOH following the testing that occurred on July 26, 2019. The cell oxygen cavity was drained of 1M KOH and then the cell was reinstalled on the test rig. The testing on July 30 lasted a 2 hr and 14 min.

C.7.1 Results

Figure C16 shows the water bath temperature, holding tank temperature, and difference in temperature between the water bath and the holding tank versus elapsed time, and the cell water temperature. The water bath temperature setpoint was set to 75 °C. The recirculation between the water bath and the holding tank was adjusted to approximately 1000 cc/min, and the water flow through the electrolysis cell was adjusted to 50 cc/min. The water bath reached 63.2 °C during the 2 hr and 14 min of testing. The holding tank reached 55.6 °C during the test. Figure C16 also shows the difference in temperature between the water bath and the holding tank reached 7.5 °C. The cell temperature reached 50.6 °C during the test.

Figure C17 shows the cell current and cell voltage versus elapsed time. The cell current was initially adjusted to about 1.4 A with a cell voltage of 1.76 VDC. The cell current was increased in steps, eventually reaching 13.5 A and a cell voltage of 1.89 VDC. The test was stopped at 2 hr 14 min of testing. This cell performance was much better than was observed in previous tests. This significant improvement in cell performance is attributed to the pre-conditioning with the 1M KOH soaking for several days prior to the testing on July 30, 2019. It was also concluded that the Mars ISRU water mixture was electrolyzed by the cell without any detrimental effects to the cell. After testing the cell was removed from the test rig and the cell oxygen cavity was flooded with 1M KOH to ensure the cell was rehydrated.

C.8 Cell Testing Data—August 1, 2019

The testing on August 1, 2019 lasted a little 4 hr and 57 min. The cell was operated with the Mars ISRU water mixture (without chlorates) that was used July 30, 2019. The cell was pre-conditioned by flooding the oxygen cavity of the cell with 1M KOH after the testing was completed on July 30, 2019. The cell performance was better than what was obtained during testing on July 30, 2019. The peak current during the August 1, 2019 testing was 16.5 A at 1.88 VDC while the peak current was 13.5 A peak at 1.89 VDC during the July 30, 2019 testing. The pre-conditioning appears to be very important to achieving good cell performance.

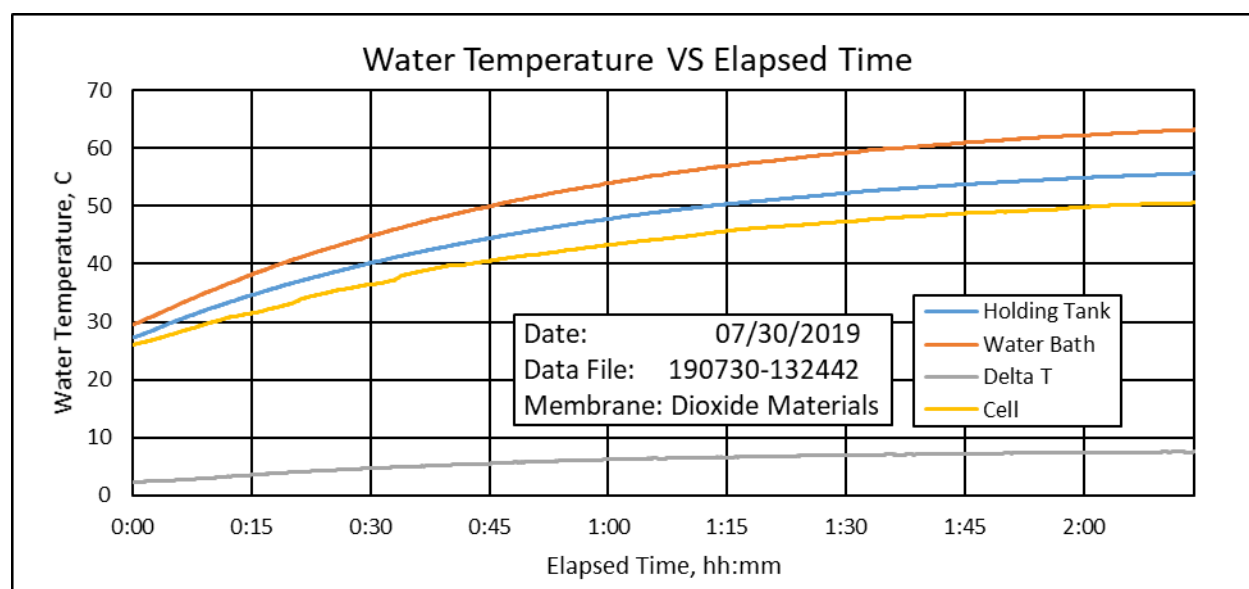


Figure C16.—Water Temperature vs. Elapsed Time 07/30/2019.

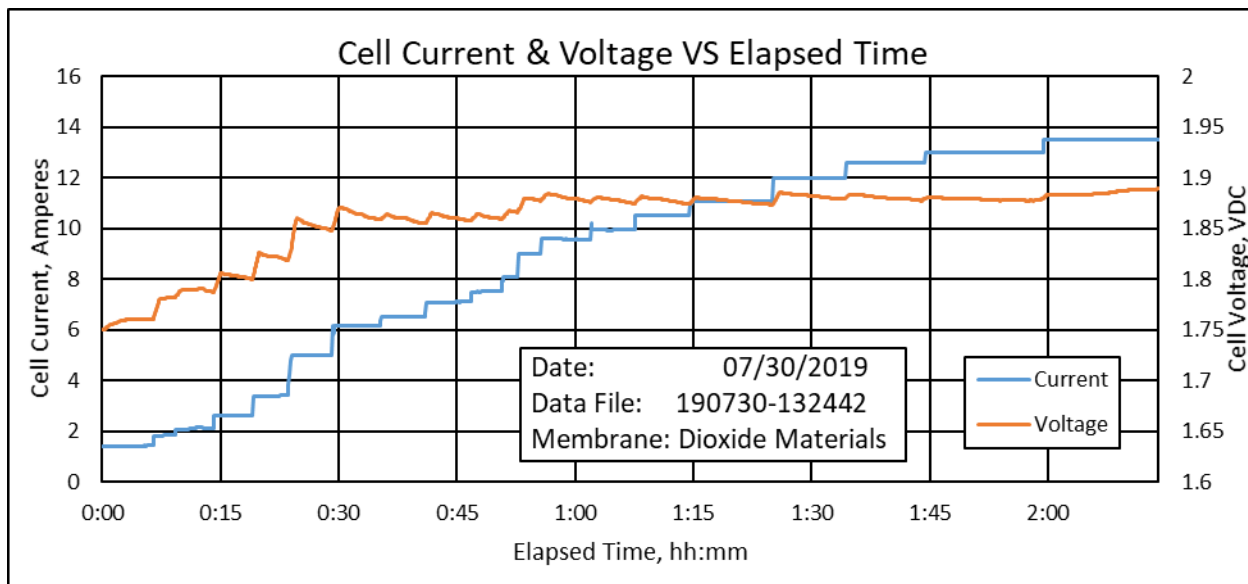


Figure C17.—Cell Current & Voltage vs. Elapsed Time 07/30/2019.

C.8.1 Results

Figure C18 shows the water bath temperature, holding tank temperature, and difference in temperature between the water bath and the holding tank versus elapsed time, and the cell water temperature. The water bath temperature setpoint was set to 75 °C. The recirculation between the water bath and the holding tank was adjusted to approximately 1000 cc/min, and the water flow through the electrolysis cell was adjusted to 50 cc/min. The water bath reached 65.5 °C during the 4 hr and 57 min of testing. The holding tank reached 57.8 °C during the test. Figure C18 also shows the difference in temperature between the water bath and the holding tank reached 7.7 °C. The cell temperature reached 52.8 °C during the test.

Figure C19 shows the cell current and cell voltage versus elapsed time. The cell current was initially adjusted to about 2.0 A with a cell voltage of 1.76 VDC. Over the next 1 hr and 51 min the current was gradually raised to 16.5 A and a cell voltage of 1.88 VDC. During this period on five occasions the cell pushed a small slug of water out of the cell’s oxygen exit port. This was an indication that the cell had sufficient water and was not in danger of drying out.

At 2 hr and 6 min into the test the current was lowered to 15.5 A and the cell voltage went dropped to 1.87 VDC. At 2 hr and 16 min into the test the current was lowered to 14.5 A and the cell voltage stayed at 1.87 VDC. At 3 hr and 45 min into the test the current was lowered to 13.5 A and the cell voltage went dropped to 1.86 VDC. At 4 hr and 19 min into the test the current was lowered to 12.5 A and the cell voltage stayed at 1.86 VDC. The current remained at 12.5 A until the test was stopped at 4 hr 57 min into the test.

After completing the test the cell was rehydrated by flooding the oxygen compartment with 1M KOH.

The hydrogen and oxygen flow exiting the cell were measured with a soap bubble flowmeter when the cell current was at 15.5 A and again when the current was 13.5 A. The measured gas flow rates are compared against the theoretical flow rates in Table C8. As was seen with earlier tests, the measured oxygen flow rate was essentially 100% of the theoretical rate and the hydrogen was about 96 to 97% of the theoretical flow rate.

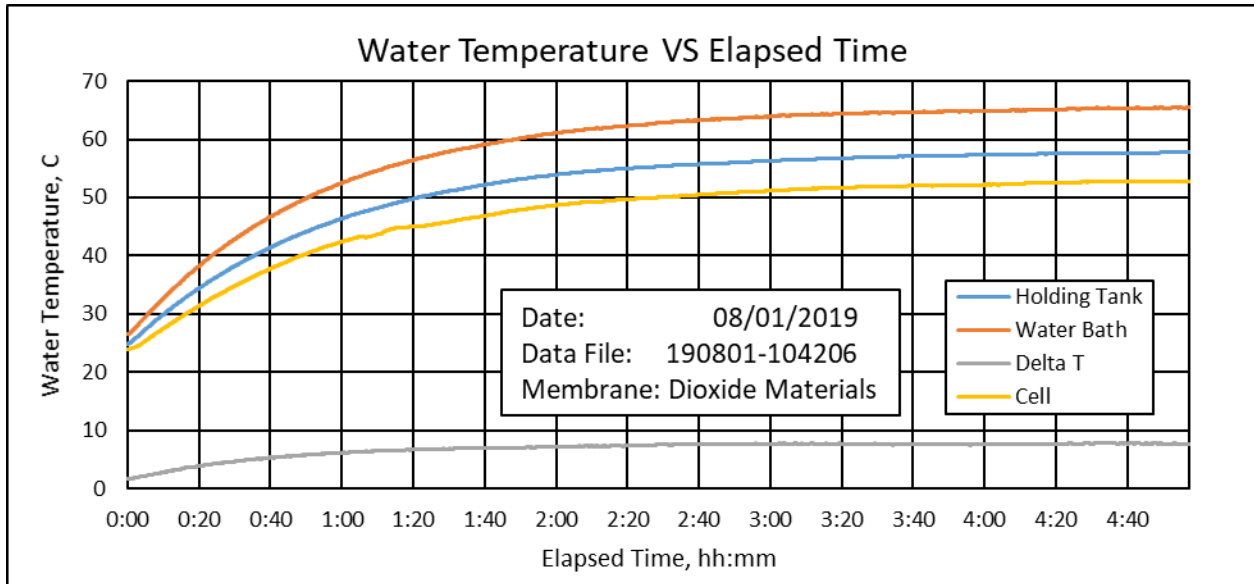


Figure C18.—Water Temperature vs. Elapsed Time 08/1/2019.

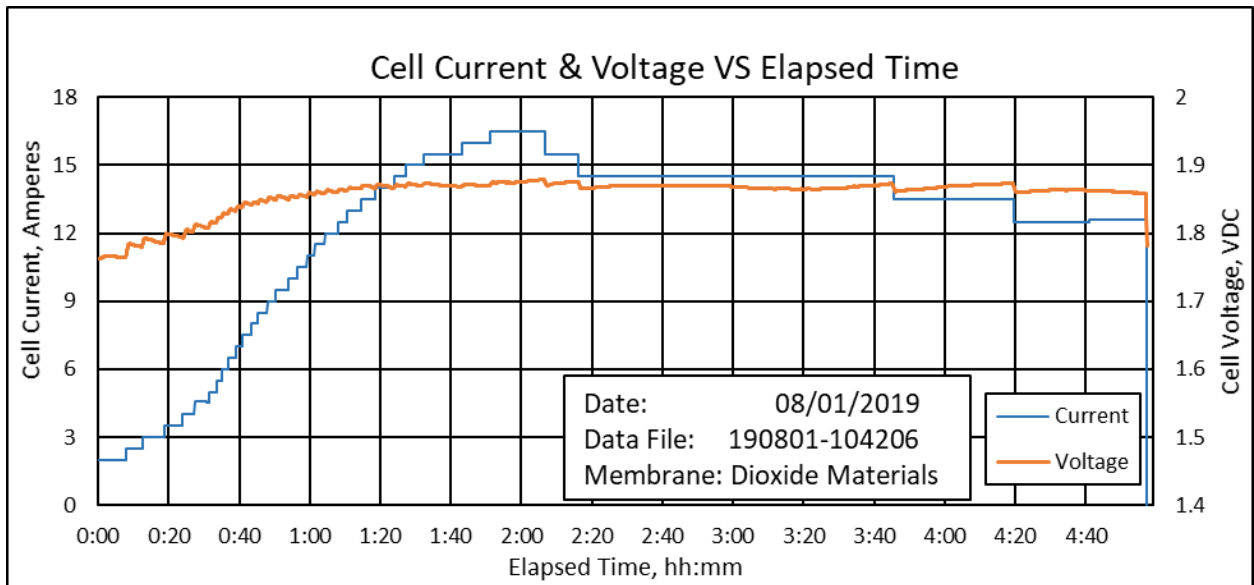


Figure C19.—Cell Current & Voltage vs. Elapsed Time 08/1/2019.

TABLE C8.—ANODE (OXYGEN) SIDE AND CATHODE (HYDROGEN) SIDE

Anode (Oxygen) Side								
Cell	Cell	Water	Oxygen	Oxygen	Total Anode	Calculated	Measured	Estimated
Current	Current Density	Consumption	Flow	Flow	Flow	Time to	Time to	Current
Amperes	mA/cm ²	ml/min	gms/min	cm ³ /min	cm ³ /min	flow 25cc	flow 25cc	Efficiency
						seconds	seconds	%
15.50	155.0	0.087	0.08	60.86	62.82	23.88	24.15	98.87
15.50	155.0	0.087	0.08	60.86	62.82	23.88	24.03	99.36
15.50	155.0	0.087	0.08	60.86	62.82	23.88	24.03	99.36
13.50	135.0	0.076	0.07	53.00	54.72	27.41	27.53	99.58
13.50	135.0	0.076	0.07	53.00	54.72	27.41	27.53	99.58
Cathode (Hydrogen) Side								
Cell	Cell	Water	Hydrogen	Hydrogen	Total Cathode	Calculated	Measured	Estimated
Current	Current Density	Consumption	Flow	Flow	Flow	Time to	Time to	Current
Amperes	mA/cm ²	ml/min	gms/min	cm ³ /min	cm ³ /min	flow 25cc	flow 25cc	Efficiency
						seconds	seconds	%
15.5	155	0.087	0.010	121.71	125.64	11.94	12.28	97.22
15.5	155	0.087	0.010	121.71	125.64	11.94	12.38	96.43
15.5	155	0.087	0.010	121.71	125.64	11.94	12.44	95.97
15.5	155	0.087	0.010	121.71	125.64	11.94	12.41	96.20
13.5	135	0.076	0.008	106.01	109.43	13.71	14.27	96.06
13.5	135	0.076	0.008	106.01	109.43	13.71	14.19	96.60
13.5	135	0.076	0.008	106.01	109.43	13.71	14.26	96.12
Ambient Laboratory Environment 25C; 1.0 atm					Cell Temperature 40C			

C.9 Cell Testing Data—August 6, 2019

The testing on August 6, 2019 lasted a 2 hr and 43 min. The cell was operated with the Mars ISRU water mixture with the chlorates that were not used in previous tests. The cell was pre-conditioned by flooding the oxygen cavity of the cell with 1M KOH after the testing was completed on August 1, 2019. The cell performance was similar to what was obtained during testing on August 1, 2019. The peak current during the August 6, 2019 testing was 15.6 A at 1.87 VDC. The addition of the chlorates missing from the previous test did not affect the cell performance. The test was stopped when no gases were observed exiting the cell’s exhaust/vent lines.

C.9.1 Results

Figure C20 shows the water bath temperature, holding tank temperature, and difference in temperature between the water bath and the holding tank versus elapsed time, and the cell water temperature. The water bath temperature setpoint was set to 75 °C. The recirculation between the water bath and the holding tank was adjusted to approximately 1000 cc/min, and the water flow through the electrolysis cell was adjusted to 50 cc/min. The water bath reached 64.7 °C during the 2 hr and 43 min of

testing. The holding tank reached 56.9 °C during the test. Figure C20 also shows the difference in temperature between the water bath and the holding tank reached 7.9 °C. The cell temperature reached 50.9 °C during the test.

Figure C21 shows the cell current and cell voltage versus elapsed time. The cell current was initially adjusted to about 0.5 A with a cell voltage of 1.67 VDC. Over the next 1 hr and 9 min the current was gradually raised to 15.5 A and a cell voltage of 1.87 VDC. During this period on two occasions the cell pushed a small slug of water out of the cell's oxygen exit port. This was an indication that the cell had sufficient water and was not in danger of drying out.

At 1 hr and 37 min into the test the current was lowered to 15.0 A and the cell voltage stayed at 1.87 VDC. At 1 hr and 42 min into the test the current was lowered to 14.5 A and the cell voltage stayed at 1.87 VDC. At 1 hr and 46 min into the test the current was lowered to 14.0 A and the cell voltage stayed at 1.87 VDC. At 1 hr and 51 min into the test the current was lowered to 13.5 A and the cell voltage stayed at 1.87 VDC. At 1 hr and 58 min into the test the current was lowered to 13.0 A and the cell voltage stayed at 1.87 VDC. At 2 hr and 13 min into the test the current was lowered to 12.5 A and the cell voltage stayed at 1.87 VDC. At 2 hr and 21 min into the test the current was lowered to 12.2 A and the cell voltage stayed at 1.87 VDC. At 2 hr and 31 min into the test the current was lowered to 12.0 A and the cell voltage stayed at 1.87 VDC. The current remained at 12.0 A until 2 hr 43 min into the test. At this point it was noticed that no hydrogen or oxygen was coming out of the exhaust/vent lines connected to the cell. The test was immediately stopped and the current turned off. It was discovered that a crack in one of the endplates was allowing gas to escape the cell without going through the cell's exhaust/vent lines.

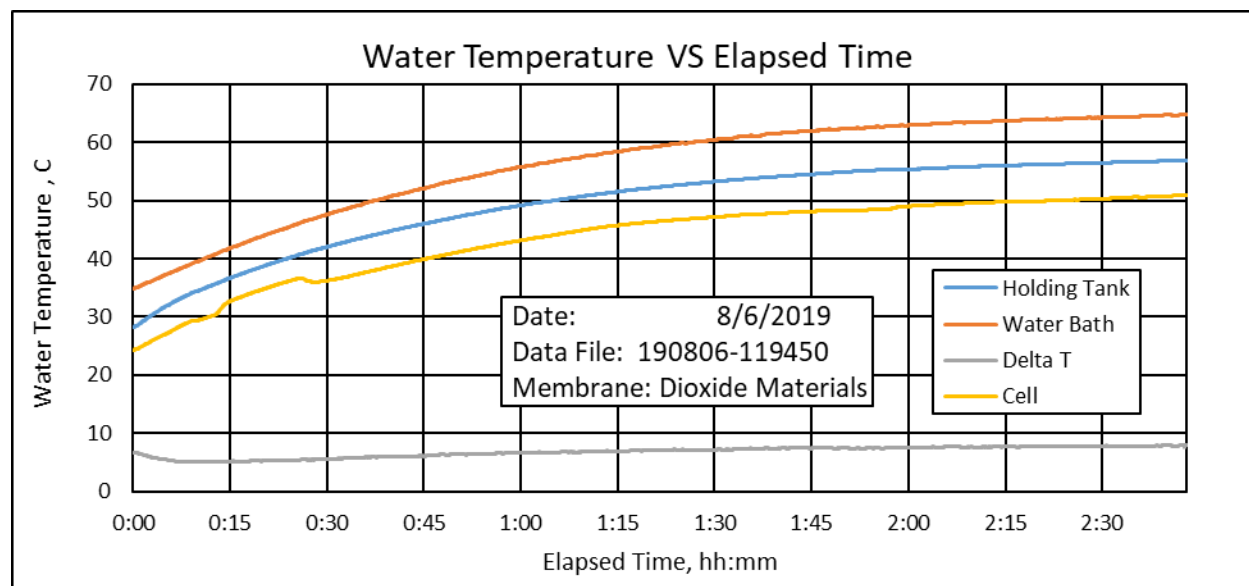


Figure C20.—Water Temperature vs. Elapsed Time 8/6/2019.

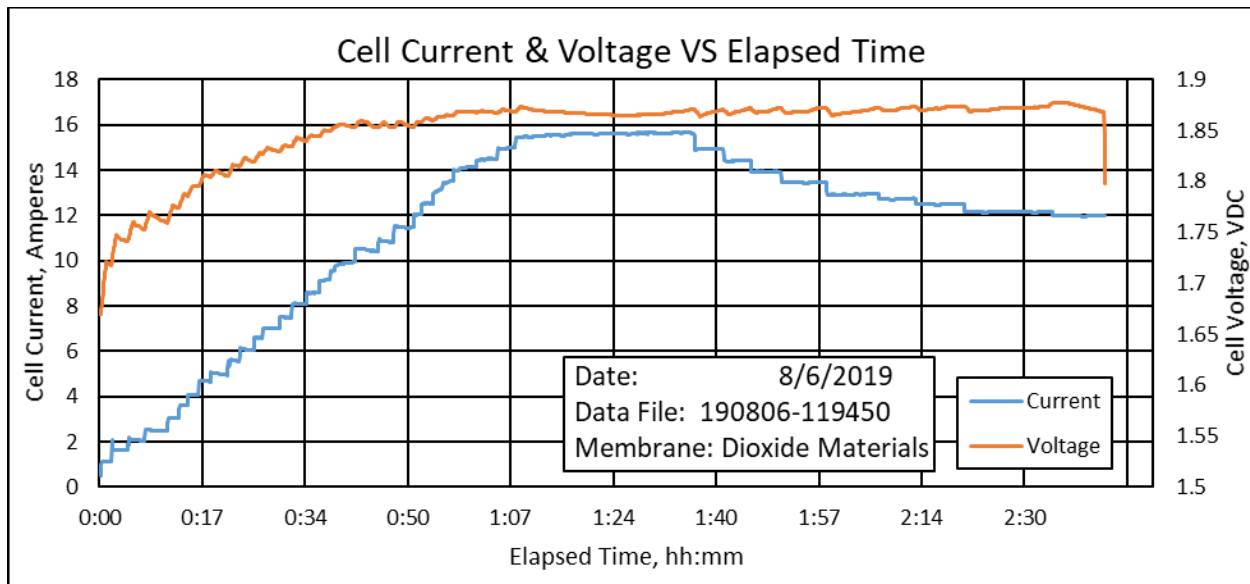


Figure C21.—Cell Current & Voltage vs. Elapsed Time 08/6/2019.

C.10 Cell Testing Data—October 2, 2019

The testing on August 6, 2019 ended when no gases were observed exiting the cell’s exhaust/vent lines. One of the cell’s endplates had developed a crack that allowed gases to leak out of the cell instead of exiting the cell through the cell’s gas exhaust/vent lines. During the endplate replacement the cell’s electrodes and membrane were damaged and could not continue to be used.

The cell was rebuilt with new electrodes and a new/different membrane from a different manufacturer. The testing on October 2 2019 was the first testing using the W7energy alkaline ion exchange membrane which was made of Poly(aryl piperidinium) and had a product identification of PAP-TP-85. The membrane used in this test, and subsequent tests was cut from a sample sent to NASA. The membrane sample thickness was 60 μm (approximately 0.0025 in.). The chemical structure of the PAP-TP-85 membrane is shown in Figure C22.

The testing on October 2, 2019 lasted a 1 hr and 8 min. The cell was operated with the Mars ISRU water mixture with the chlorates. The cell membrane was conditioned prior to cell assembly by soaking the membrane in 1M KOH for 24 hr.

C.10.1 Results

Figure C23 shows the water bath temperature, holding tank temperature, and difference in temperature between the water bath and the holding tank versus elapsed time, and the cell water temperature. The water bath temperature setpoint was set to 75 °C. The recirculation between the water bath and the holding tank was adjusted to approximately 1000 cc/min, and the water flow through the electrolysis cell was adjusted to 50 cc/min. The water bath reached 58.6 °C during the 1 hr and 8 min of testing. The holding tank reached 50.9 °C during the test. Figure C23 also shows the difference in temperature between the water bath and the holding tank reached 7.7 °C. The cell temperature reached 45.5 °C during the test.

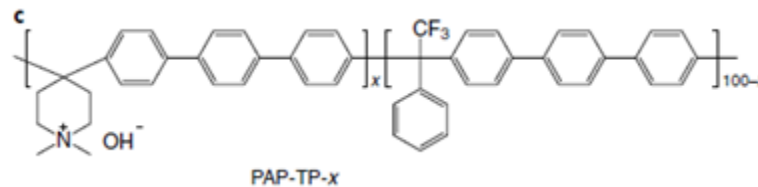


Figure C22.—Chemical Structure of the PAP Anion Exchange Membrane Family.

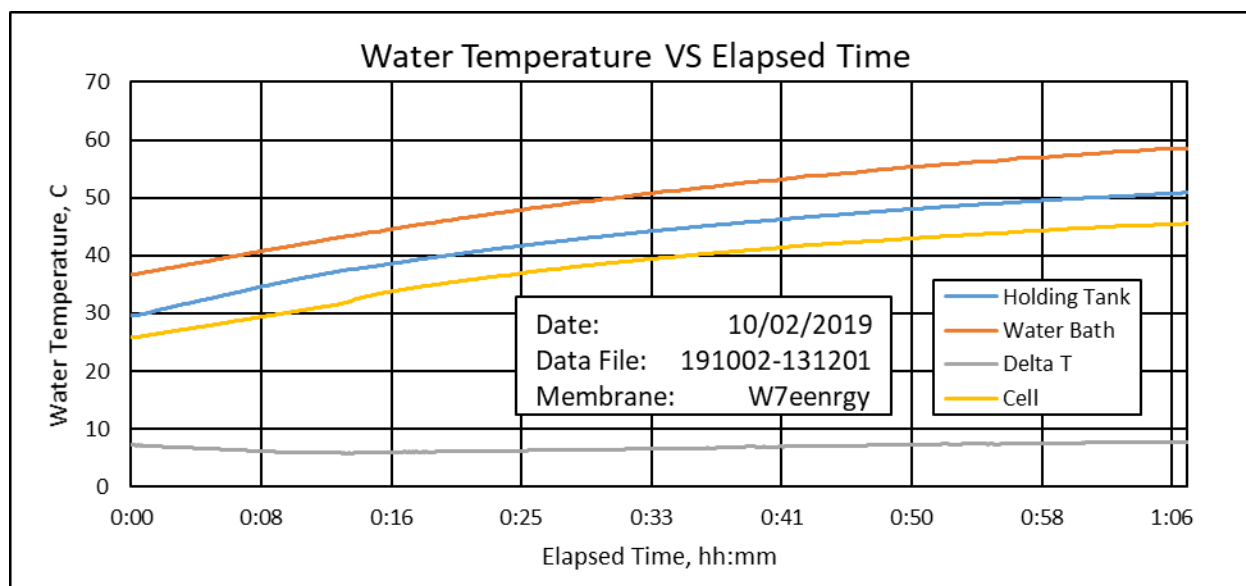


Figure C23.—Water Temperature vs. Elapsed Time 10/2/2019.

Figure C24 shows the cell current and cell voltage versus elapsed time. The cell current was initially adjusted to about 0.7 A at 2 min and 20 sec into the test. The cell did not increase to its electrolysis voltage for 30 sec (2 min 50 sec into the test). At 2 min and 50 sec with the current at 0.18 A the cell reached its electrolysis voltage of 1.57 VDC. The current was increased to 0.28 A with a cell voltage of 1.83 VDC at 3 min and 15 sec into the test. The current was gradually increased to 0.31 A over the next 2 min and 15 sec (6 min 0 sec into the test) and the cell voltage increased to 1.99 VDC. The current was maintained at 0.31 A for the next 4 min 45 sec (10 min 45 sec into the test) and the cell voltage climbed to 2.08 VDC. At this point the current was decreased to 0.09 A and the cell voltage decreased to 2.04 VDC. The current was maintained at 0.09 A over the next 21 min (25 min 45 sec into the test) and the cell voltage decreased to 1.81 VDC. The current was then increased 0.30 A and the cell voltage increased to 1.83 VDC. The current was maintained at 0.30 A over the next 2 min 30 sec while the cell voltage increased to 2.06 VDC. At 28 min 30 sec the current was decreased to 0.2 A and the cell voltage decreased to 2.04 VDC. The current was maintained at 0.2 A for 7 min 5 sec (35 min 30 sec into the test) and the cell voltage decreased to 1.98 VDC. At 35 min 50 sec the current was reduced to 0.05 A and the cell voltage decreased to 1.95 VDC. The current was maintained at 0.05 A for the next 24 min 55 sec (until 60 min 45 sec into the test) and the cell voltage decreased to 1.71 VDC. At 60 min 50 sec the current was increased 0.22 A and the cell voltage increased to 1.73 VDC. The current was maintained at 0.22 A for the next 6 min 45 sec (until 67 min 35 sec into the test) and the cell voltage increased to 2.05 VDC. At 57 min 35 sec the current was turned off and the test stopped.

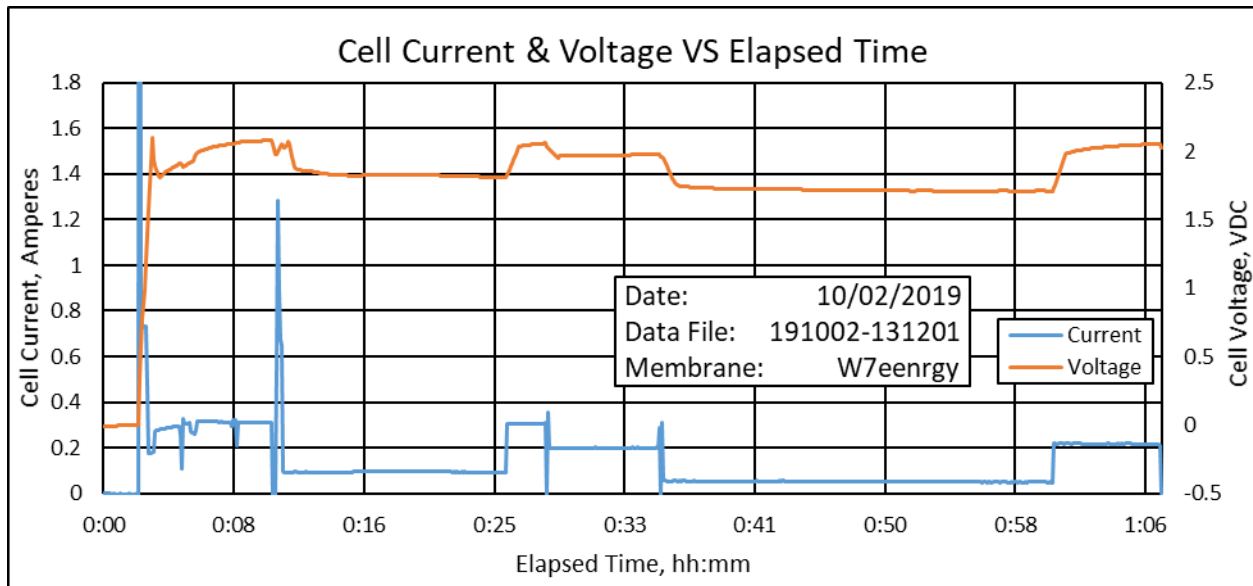


Figure C24.—Cell Current & Voltage vs. Elapsed Time 10/2/2019.

The substantial swings in cell voltage with the small changes in current indicates that the cell is quite sensitive to membrane hydration.

C.11 Cell Testing Data—October 3, 2019

The testing on October 3, 2019 was the second test using the W7energy alkaline ion exchange membrane. The testing on October 3, 2019 lasted a 1 hr and 30 min. The cell was operated with the Mars ISRU water mixture with the chlorates.

C.11.1 Results

Figure C25 shows the water bath temperature, holding tank temperature, and difference in temperature between the water bath and the holding tank versus elapsed time, and the cell water temperature. The water bath temperature setpoint was set to 75 °C. The recirculation between the water bath and the holding tank was adjusted to approximately 1000 cc/min, and the water flow through the electrolysis cell was adjusted to 50 cc/min. The water bath reached 60.2 °C during the 1 hr and 30 min of testing. The holding tank reached 52.2 °C during the test. Figure C25 also shows the difference in temperature between the water bath and the holding tank reached 8.0 °C. The cell temperature reached 47.1 °C during the test.

Figure C26 shows the cell current and cell voltage versus elapsed time.

The cell current was initially adjusted to about 0.21 A and the cell instantly polarized to 1.64 VDC. The current was maintained at 0.21 A for the next 27 min 5 sec and the cell voltage stayed at 1.64 VDC. At this point the current was decreased to 0.5 A and the cell voltage increased to 1.65 VDC. The current was maintained at 0.5 A over the next 41 min 20 sec (68 min 25 sec into the test) and the cell voltage increased to 1.70 VDC. At this point the current was increased to 1.23 A and the cell voltage increased to 1.74 VDC. The current was maintained at 1.23 A over the next 20 min 25 sec (88 min 50 sec into the test) and the cell voltage increased to 1.81 VDC. The current was gradually reduced to 0.0 A over the next 1 min 20 sec (90 min and 10 sec into the test).

There were no substantial swings in cell voltage with the small changes in current that was seen during the test October 2, 2019.

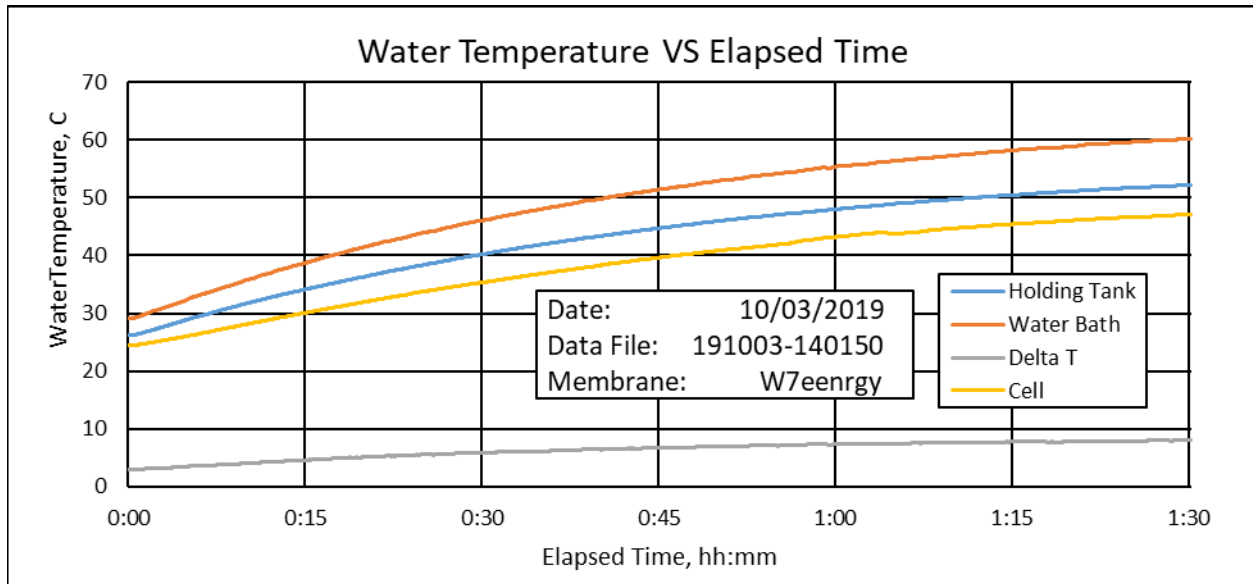


Figure C25.—Water Temperature vs. Elapsed Time 10/3/2019.

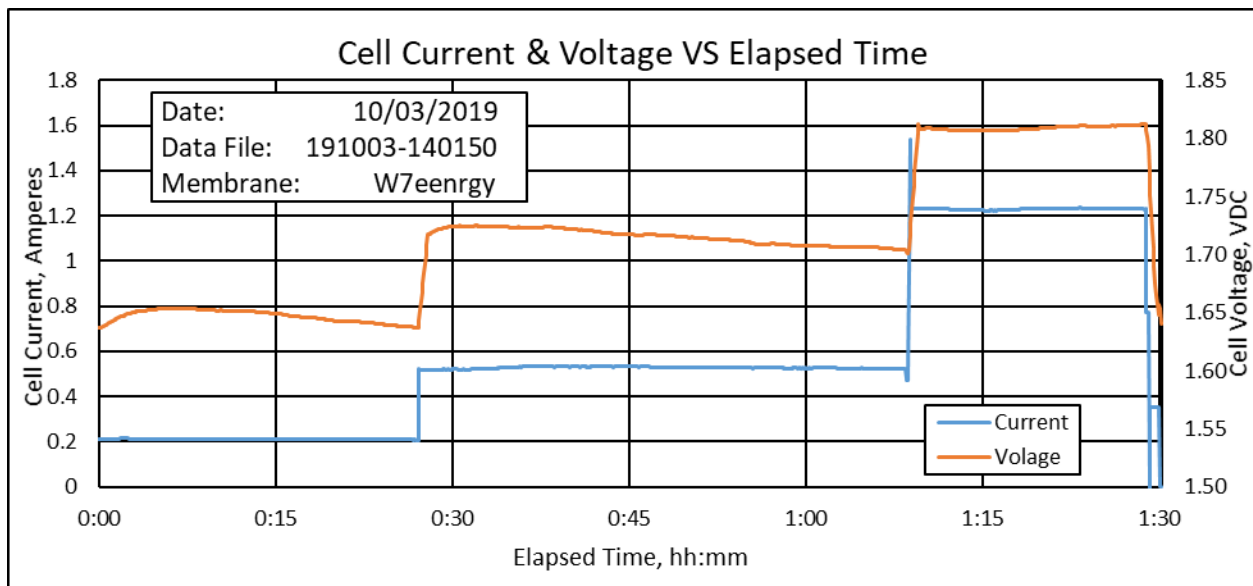


Figure C26.—Cell Current & Voltage vs. Elapsed Time 10/3/2019.

C.12 Cell Testing Data—October 23, 2019

The testing on October 23, 2019 was the third test using the W7energy alkaline ion exchange membrane. The testing on October 23, 2019 lasted 1 hr and 34 min. The cell was operated with the Mars ISRU water mixture with the chlorates.

C.12.1 Results

Figure C27 shows the water bath temperature, holding tank temperature, and difference in temperature between the water bath and the holding tank versus elapsed time, and the cell water temperature. The water bath temperature setpoint was set to 75 °C. The recirculation between the water bath and the holding tank was adjusted to approximately 1000 cc/min, and the water flow through the

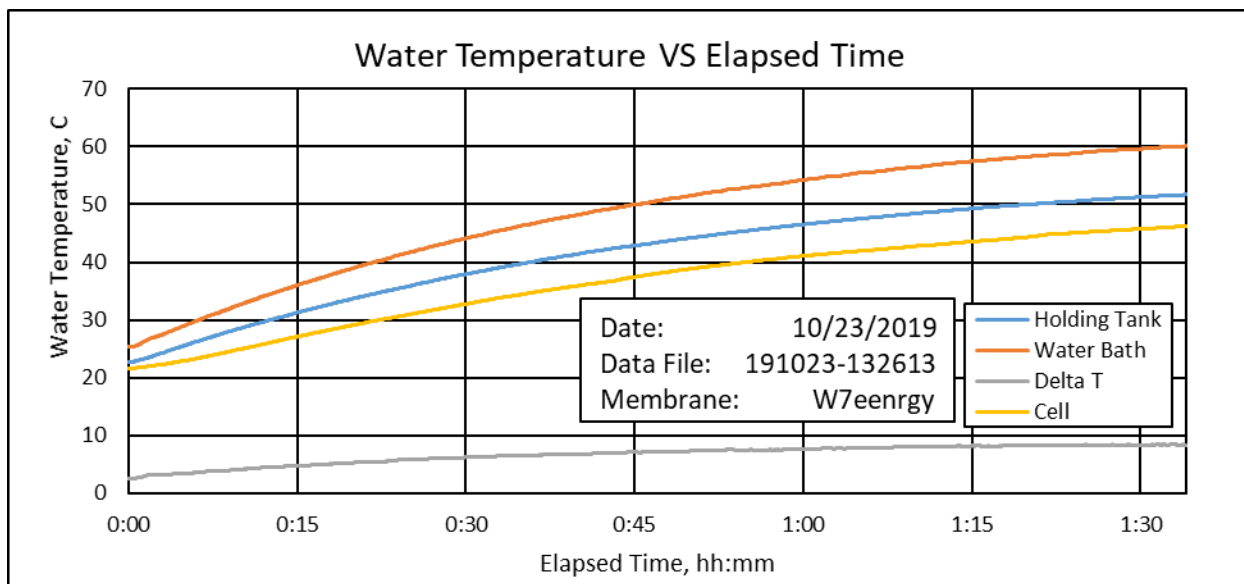


Figure C27.—Water Temperature vs. Elapsed Time 10/23/2019.

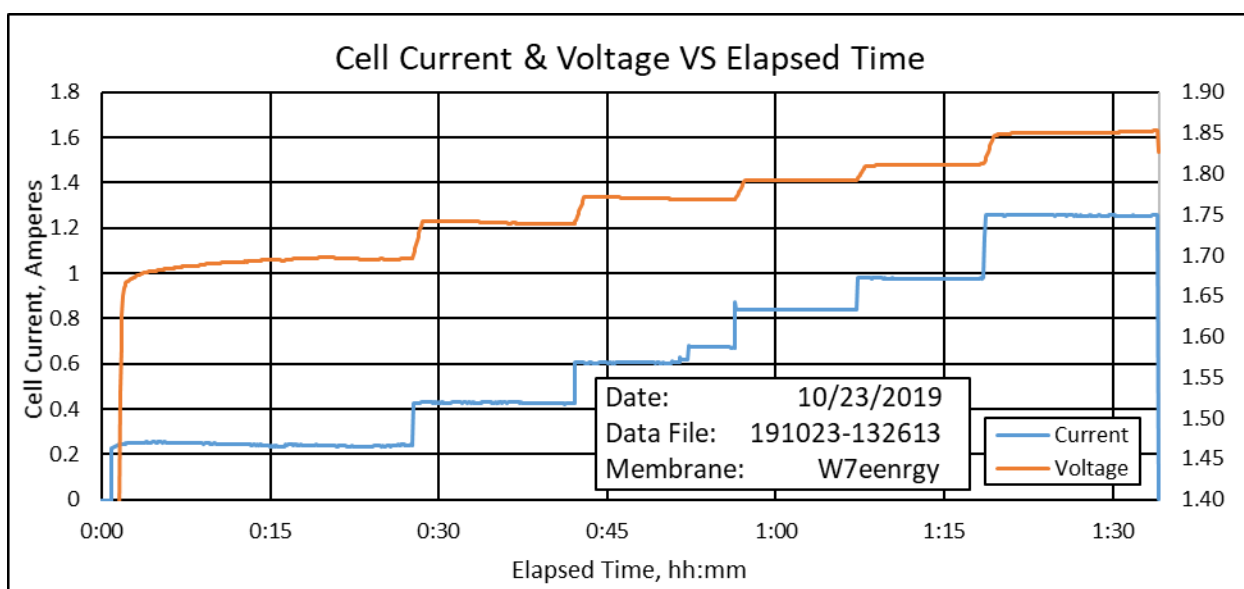


Figure C28.—Cell Current & Voltage vs. Elapsed Time 10/23/2019.

electrolysis cell was adjusted to 50 cc/min. The water bath reached 60.1 °C during the 1 hr and 34 min of testing. The holding tank reached 51.7 °C during the test. Figure C27 also shows the difference in temperature between the water bath and the holding tank reached 8.4 °C. The cell temperature reached 46.2 °C during the test.

Figure C28 shows the cell current and cell voltage versus elapsed time.

The cell current was initially adjusted to about 0.24 A and the cell polarized to 1.65 VDC after 60 sec. The current was maintained at 0.24 A for the next 26 min 45 sec and the cell voltage stayed at 1.70 VDC. At this point the current was increased to 0.42 A and the cell voltage increased to 1.71 VDC. The current was maintained at 0.42 A over the next 15 min 25 sec (42 min 10 sec into the test) and the cell voltage increased to 1.74 VDC.

At this point the current was increased to 0.61 A and the cell voltage increased to 1.77 VDC.

The current was maintained at 0.61 A over the next 10 min 0 sec (52 min 10 sec into the test) and the cell voltage stayed at 1.77 VDC. The current was increased to 0.67 A and the cell voltage stayed at 1.77 VDC. The current was maintained at 0.67 A over the next 4 min 15 sec (56 min 25 sec into the test) and the cell voltage stayed at 1.77 VDC. The current was increased to 0.84 A and the cell voltage increased to 1.78 VDC. The current was maintained at 0.84 A over the next 10 min 50 sec (67 min 15 sec into the test) and the cell voltage increased to 1.79 VDC. The current was increased to 1.0 A and the cell voltage increased to 1.79 VDC. The current was maintained at 1.0 A over the next 11 min 15 sec (78 min 30 sec into the test) and the cell voltage increased to 1.81 VDC. The current was increased to 1.25 A and the cell voltage increased to 1.83 VDC. The current was maintained at 1.25 A over the next 15 min 30 sec and the cell voltage increased to 1.85 VDC. At 1 hr 34 min into the test the test was stopped.

The performance during this test was very similar to the cell performance observed on October 3, 2019. Additional membrane conditioning might improve the cell performance.

Reference

1. “The effect of membrane on an alkaline water electrolyzer,” Zengcai Liu, Syed Dawar Sajjad, Yan Gao, Hongzhou Yang, Jerry J. Kaczur, Richard I. Masel, International Journal of Hydrogen Energy Volume 42, Issue 50, 14 December 2017, Pages 29661–29665.

